NOAA Technical Memorandum ERL SEL-46

DEPARTMENT OF COMMERCE ★ UNITED STATES OF AMERICA ★

A STUDY OF THE CAPABILITY FOR RAPID WARNINGS OF SOLAR FLARE RADIATION HAZARDS TO AIRCRAFT

PART I. FORECASTS AND WARNINGS OF SOLAR FLARE RADIATION HAZARDS

PART II. AN FAA POLAR FLIGHT SOLAR COSMIC RADIATION FORECAST/WARNING COMMUNICATION SYSTEM STUDY

Herbert H. Sauer
Garth H. Stonehocker

Space Environment Laboratory
Boulder, Colorado
April 1977

noaa NATIONAL OCEANIC AND ATMOSPHERIC ADMINISTRATION / Environmental Research Laboratories

NOAA Technical Memorandum ERL SEL-46

A STUDY OF THE CAPABILITY FOR RAPID WARNINGS OF SOLAR FLARE RADIATION HAZARDS TO AIRCRAFT

PART I. FORECASTS AND WARNINGS OF SOLAR FLARE RADIATION HAZARDS

PART II. AN FAA POLAR FLIGHT SOLAR COSMIC RADIATION FORECAST/WARNING COMMUNICATION SYSTEM STUDY

Herbert H. Sauer
Space Environment Laboratory

Garth H. Stonehocker
Office of Telecommunications

Space Environment Laboratory
Boulder, Colorado
April 1977

UNITED STATES
DEPARTMENT OF COMMERCE
Juanita M. Kreps, Secretary

NATIONAL OCEANIC AND
ATMOSPHERIC ADMINISTRATION
Robert M. White, Administrator

Environmental Research
Laboratories
Wilmot N. Hess, Director

NOAA
NATIONAL OCEANIC AND ATMOSPHERIC ADMINISTRATION
U.S. DEPARTMENT OF COMMERCE

PREFACE

Solar flares may produce radiation levels at aircraft cruising altitudes which may require action to be taken in order to reduce the radiation hazard to the crew and passengers to acceptable levels. This study examines the systems which might implement such action. This report comprises two parts.

Part I entitled "Forecasts and Warnings of Solar Flare Radiation Hazards" examines the occurrence of solar flares and solar cosmic ray events, and describes present capabilities for the forecasting and warning of such events, together with near-term expectations for improvements of such systems.

It is recognized that solar proton events are almost always associated with periods of geophysical disturbances during which, for example, UHF communications may be seriously compromised or entirely disrupted. Therefore, Part II entitled "An FAA Polar Flight Solar Cosmic Ray Radiation Forecast/Warning Communications System Study", examines current and future aeronautical communications systems in order to help determine a suitable forecast message distribution system under such disturbed conditions.

These studies were supported by the Federal Aviation Administration under Interagency Agreement DOT-FA72WAI-320.

TABLE OF CONTENTS

FIGURES

TABLES

Part I

Abstract

This part of the report provides background information on the occurrence of solar activity and the consequent sporadic production of electromagnetic and particle emissions from the sun. A summary is given of the current procedures for the forecasting of solar activity together with procedures used to verify these forecasts as currently available. A summary of current forecasting of radiation hazards as provided in support of the Concorde SST program is also given.

SOLAR FLARES

1. Introduction

A large body of literature exists on the subject of solar activity and, in particular, studies of solar flares and their consequences (see for example, Svetska, 1976; or for current research in Solar Terrestrial Physics, Williams, 1976). The well-known 11 year solar cycle is most easily characterized by examining a plot of mean sunspot number as function of time (Figure 1). The occurrence of solar flares is well correlated with the level of solar activity.

2. Optical Emission

Optical solar flares are detected as sudden intense brightenings of active regions at the wavelength of the Hydrogen alpha (Hα) absorption line, although the larger events may be observable in white light. The size of a flare has historically been classified according to the apparent brightness together with an assessment of the area of brightening expressed in units of millionths of the solar disc.

Optical observations of solar flares have been made since 1859, when Carrington and Hodges first observed solar flares in white light. More sophisticated instrumentation has since been developed which allow observations to be made at discrete wavelengths, permitting different levels of the solar surface to be examined. Such instruments allow observation of material motions through measurements of Doppler shifts at the observing wavelength, and permit determination of magnetic fields in the vicinity of solar active regions through study of Zeeman Effect spectral shifts.

The optical brightenings of the flare process are, however, only the visible manifestations of dynamic magneto-plasma processes involving emission of a broad range of electromagnetic radiation as well as emission of charged particles.

The frequency of occurrence of solar cosmic ray events follows the eleven year cycle of general solar activity except that the peak cosmic ray occurrence tends to be somewhat before or after the peak solar activity. Figure 2 (from Webber, 1964) indicates the correlation between the frequency of solar cosmic ray events and solar activity. It will be seen that the yearly frequency of events follows quite closely the average sunspot number.

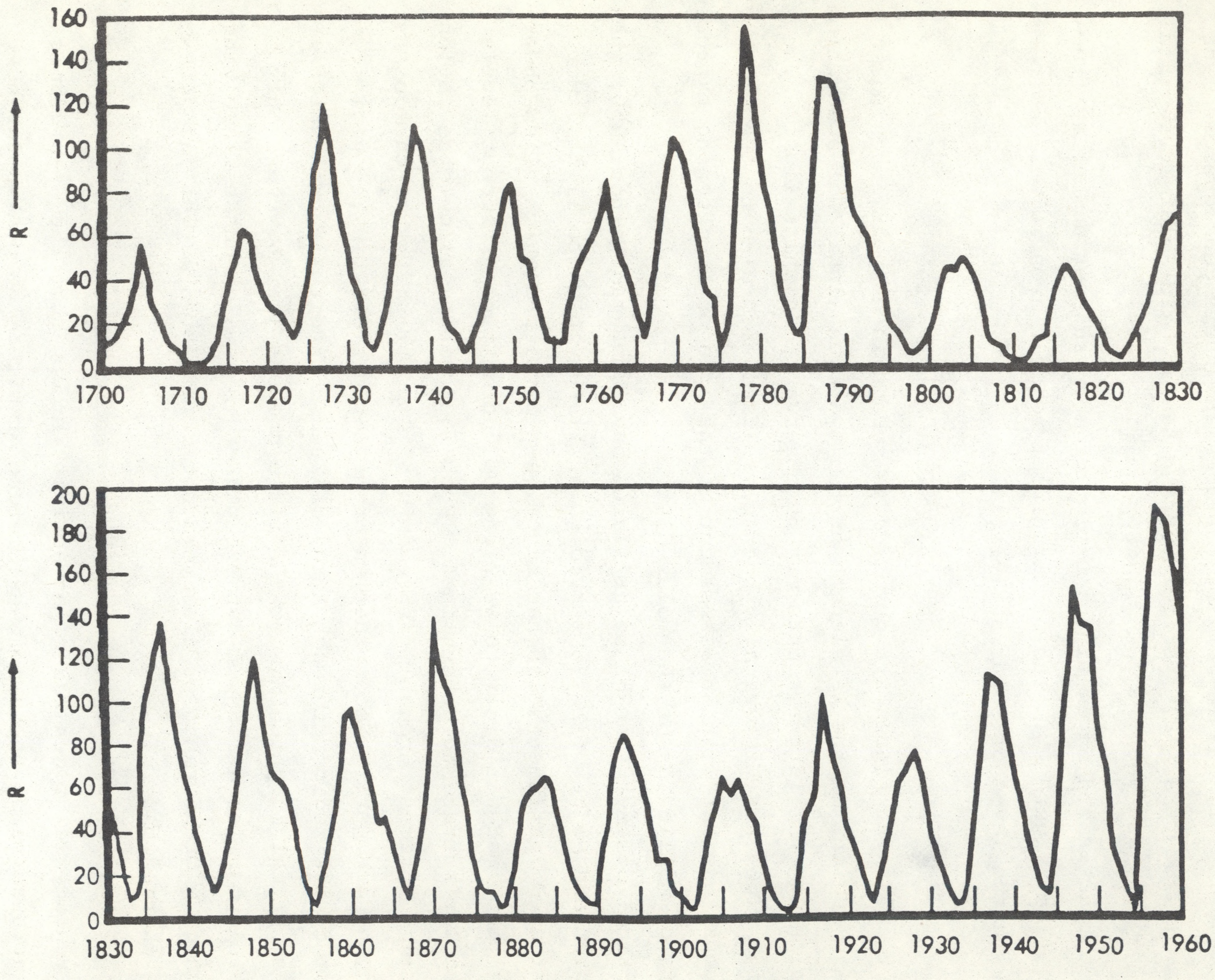

Figure 1 Annual mean sunspot number R for the years 1700 to 1960

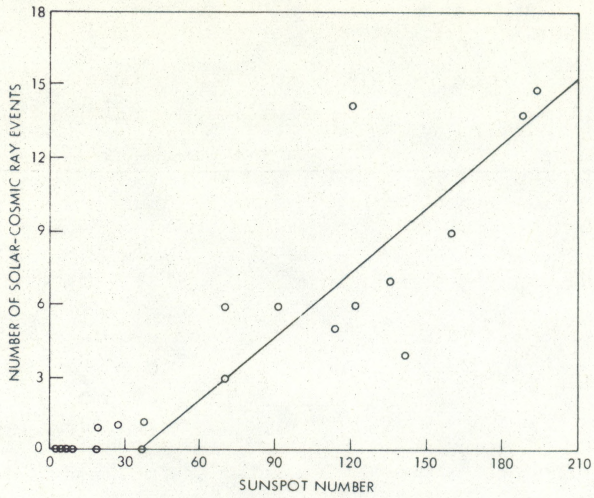

FIGURE 2 **Yearly number of solar cosmic ray events observed as a function of yearly average sunspot number.**

The individual events are clearly related to solar flares on the sun. The various optical and radio emissions from the flares are of importance in understanding the production of cosmic rays and in general, the greater the electromagnetic wave emission from a flare, the higher the probability that the flare will produce solar cosmic rays. Figure 3 (Webber, 1964) clearly illustrates this association with respect to centimeter radio emission. Plotted are integrated solar cosmic ray intensity greater than 30 MeV, against the integrated radio emission at 10,000 MHz.

Table I comprises a list of the larger solar proton events that have occurred since 1956, for which at least reasonable estimates of the fluxes greater than 30 MeV are available (McDonald, 1963; King, 1972, SESC, 1974). This choice of threshold while lower than desirable for consideration of radiation hazard, was made necessary by reducing the extrapolations and interpolations of existing data. Included in the table are the concurrent measurements of 30 MHz riometer absorption that have been obtained.

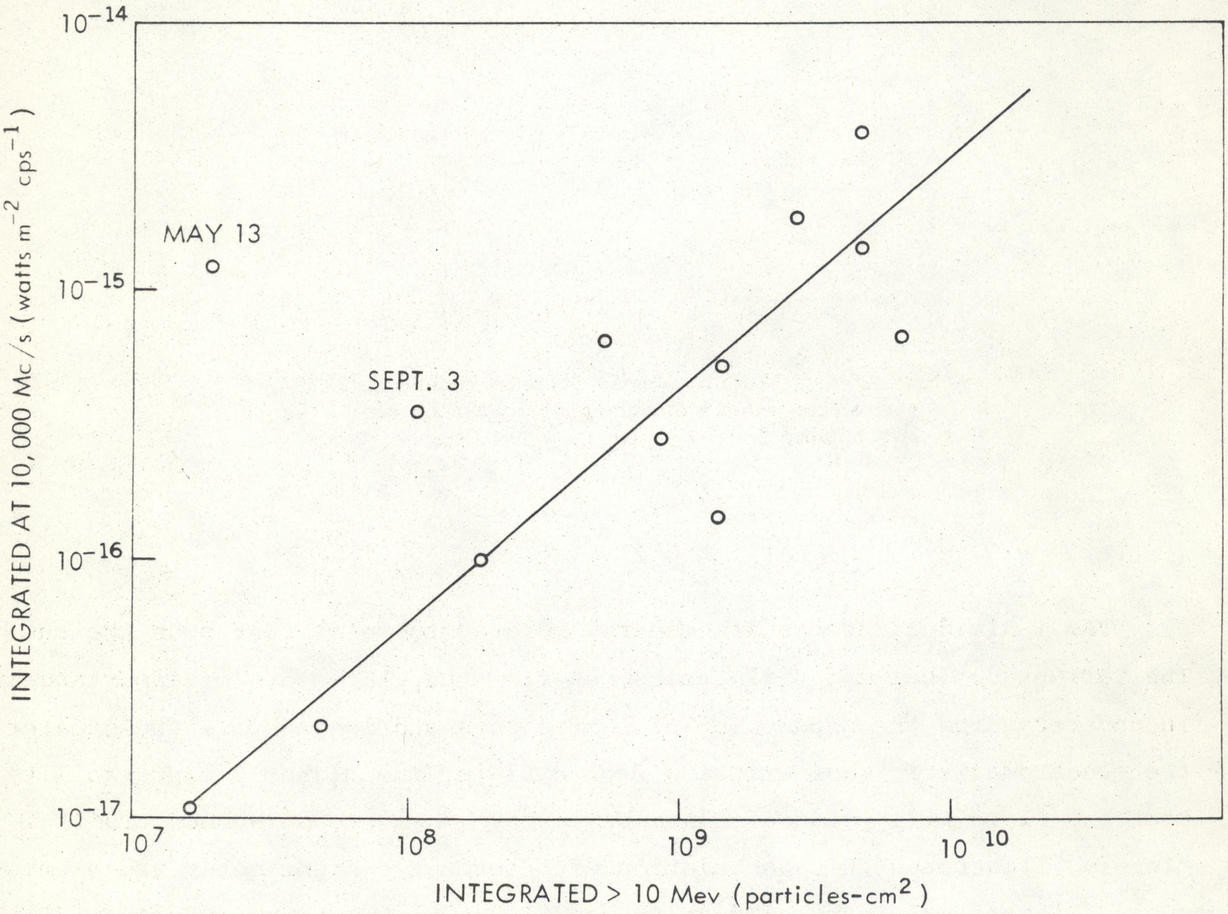

Integrated radio emission at 10,000 Mc/s versus integrated intensity of solar particles above 10 Mev at the earth for various events.

Figure 3

Table 1

Solar Proton Event Occurrences

Year	Date	Peak Flux > 30 MeV $(cm^2 sec\ ster)^{-1}$	Peak 30 MHz Abs. (db)
1956	Feb. 23	6200	13
	Aug. 31	-	4.9
1957	Jun 20	∿ 2500	4.1
	July 3	-	9.2
	Aug. 29	∿ 250	2.0
	Oct. 20	-	7.8
1958	Feb. 9	-	3.2
	Mar. 23	∿ 1350	3.2
	July 7	∿ 1750	23.7
	Aug. 16	200	12.1
	Aug. 22	500	10.6
	Aug. 26	1100	16.6
1959	May 10	∿ 7000	22
	July 10	4000	20
	July 14	∿ 11000	23
	July 16	∿ 17000	21
1960	Apr. 1	50	3.6
	Apr. 5	40	3.0
	Apr. 28	300	2.5
	May 4	200	3.4
	May 6	∿ 75	8.7
	Sept. 3	240	2.7
	Nov. 12	120000	21.
	Nov. 15	6000	20.
	Nov. 20	1000	3
1961	July 11	20	2
	July 12	120	17
	July 18	2500	8.7
	July 20	300	2
	Sept. 10	10	2.1
	Sept. 28	30	2.9
	Nov. 10	30	2.0

1963	Apr. 15	-	2.0
	Sept. 21	7	3.1
	Sept. 26	7	4.6
1964	Mar. 16	-	1.4
1965	Febr. 5	∿ 25	1.8
1966	Mar. 23	∿ 10	1.6
	July 7	∿ 40	2.1
	Aug. 28	∿ 50	4.0
	Sept. 2	∿ 150	13
1967	Jan. 28	∿ 75	6.5
	Mar. 12	∿ 30	1.3
	May 25	32	10
	May 28	27	3
	Dec. 3	10.5	1.7
	June 9	12.4	6
	Sept. 28	19	1.2
	Oct. 4	6.3	1.8
	Oct. 31	10	5
	Nov. 18	404	12
	Dec. 4	31	4.5
1969	Feb. 25	41	2.2
	Mar. 30	13	1.4
	Apr. 12	123	12
	Nov. 2	737	14
1970	Jan. 31	6.2	3
	Mar. 6	.9	1
	Mar. 29	20.2	1.8
	July 23	.8	3.6
	Aug. 14	2.7	2.6
	Nov. 5	1.7	3.5
1971	Jan. 24	408	11.8
	Apr. 6	5	3.8
	Sept. 1	162	4.2
	May 28	2.7	1.1
	Aug. 4	21.000	720
	Aug. 7	384	

The relative infrequency of entries earlier in the table are more indicative of the availability of measurements than of the occurrence of events. By 1962, both satellite measurements of particle spectra and the availability of riometer observing sites had increased to the point where most significant events were reliably observed. The increase of reliable observations may be further implied by noting that the earlier measurements show large discrepancies with the expected and more recently confirmed relationship between flux and riometer absorption given by Kane and Masley (1972), for example:

$$A = .31 \, [J \, (> 10 \text{ MeV})]^{1/2} \tag{1}$$

where J (> 10 MeV) denotes the flux in $(\text{cm}^2 \text{ ster sec})^{-1}$, and A denotes the 30 MHZ absorption.

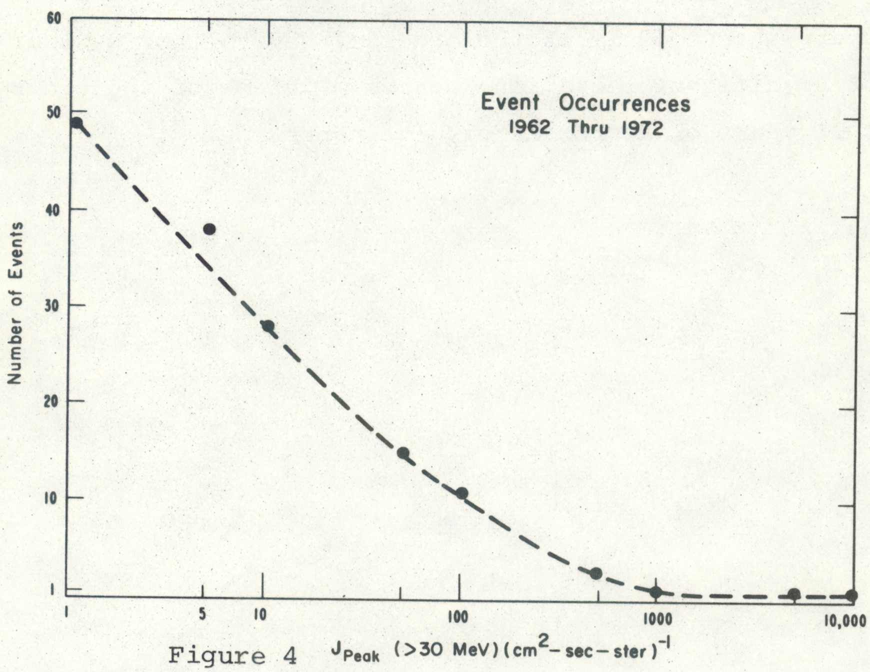

Figure 4

Figure 4 illustrates the distribution of event peak integral fluxes greater than 30 MeV for the 11-year period preceding 1973. From the standpoint of radiation hazard at aircraft altitude, interest would center on peak fluxes above 1000 cm^2, sec ster, although clearly one must consider the relative hardness of an individual event as well as the peak fluxes to make better than an order of magnitude assessment of the dose rate at altitude due to such an event. It will be seen however, that during this 11-year period only one event exceeded 1000 particles/cm^2 sec ster. This event occurred in the period Aug. 4-7, 1972 and the estimate of the peak dose rate at 60,000 feet was approximately 350 mrem/hr. The previous eleven year period included the great flare of Feb. 23, 1956 which has been estimated to have produced a dose rate at 60,000 feet of the order of 1 rem/hr, which would also have well exceeded the present arbitrary threshold of interest of 1000 part/cm^2 sec ster, one might then roughly conclude from Figure 4 that on the average there would be one or two events per solar cycle of distinct interest. Assuming, as has been the case for these events, that the duration of the peak of the event over our arbitrary threshold is of the order of several hours, that the probability of significant radiation dosages might be of the order of 10-20 hours per 11 years or approximately 1-2 parts in 10^4.

3. X-ray and Radio Emission

Concurrent with the visible brightenings, the solar flare is found to emit electromagnetic radiation from the high radio frequencies through x-ray frequencies, with the most prominent enhancements in the extreme ultraviolet (EUV) and x-ray wavelengths. These emissions most commonly continue some minutes to tens of minutes as does the optical flare brightening, however, for unusually large flares, durations of several hours have been observed.

The radio emissions have direct consequences on high to ultra high frequency (HF to UHF) communications and interference due to solar radio noise bursts was recognized as early as the 1930's with the advent of long distance HF communications. The effect of the shorter wavelength solar x-ray and EUV emissions on radio communications occurs more indirectly through the enhanced ionization produced in the earth's atmosphere.

Some understanding of the mechanisms of production of flare emissions through plasma processes such as synchrotron emission and bremstrahlung, for example, has occured since the discovery in 1946 that the sun was capable of producing large bursts of energetic particles in the flare process.

4. Solar Cosmic Radiation

Considerable progress has been made in understanding the earth's radiation environment since the discovery of cosmic rays by Hess (1912), although fifteen years were to elapse before Clay (1927), during ocean voyages between Java and Holland, found a consistently lower cosmic ray ionization near the equator and thus made the first use of the magnetic field of the earth as a charge spectrometer. This progress took the form of comprehensive studies of the radiation and magnetic fields surrounding the earth, and the phenomena resulting from their interaction. The greatest impetus to these studies was imparted by the establishment of the International Geophysical Year (July 1957 to December 1958) and, more recently, through the advent of artificial satellites which focused attention and resources on questions of geophysical interest.

The study of energetic particles emitted from the sun, solar cosmic radiation, began in detail with the great event of February 23, 1956. At that time only few cases of ground level events that could be attributed to solar activity had been observed and consequently such solar cosmic ray events were considered rare. With the development of particle counters flown to high altitudes on balloons, rockets and finally artificial earth satellites, a relatively complete picture of these events has emerged, together with a good understanding of the background plasma emission from the sun, the solar wind.

Cosmic rays emitted from the sun are primarily protons in the energy interval of some several MeV (10^6 electron volts) to several GeV (10^9 electron volts). Solar cosmic ray events occur with a frequency such that these particles may reach the near-earth environment a significant fraction of the time, but only about 1% of the time will solar particles exceed the intensity of the ubiquitous galactic cosmic rays.

The energy spectrum of these particles is usually quite steep (i.e. relatively few high energy particles), but occasionally in the so-called great events, the energy spectrum may be so flat that an appreciable flux of particles and their atmospherically produced secondaries may penetrate the entire atmosphere and produce a ground level event. Such events are clearly of importance for radiation hazard considerations at aircraft altitudes.

PREDICTION OF SOLAR FLARES AND PROTON EVENTS

1. Introduction

Space Environment Forecasting had its origins before World War II. In the late 1930's, solar geophysical data were interchanged between a few scientists for the purposes of better planning of future observing programs as well as providing a better understanding of past observations. During World War II and the following IGY period, solar geophysical data continued, however, emphasis was particularly placed on ionospheric and radio propagation aspects rather than on space environment aspects as such.

It was the events of the early space era, the launching of the first satellites and the proposed moon landings, that were directly responsible for the establishiment of the Space Environment Services Center (SESC) in what is now National Oceanic and Atmospheric Administration (NOAA). The potential radiation hazards associated with man's incursion into "space" led to the development of a real-time, operational space environment forecast system. The program is a melding of the resources of the Department of Defense, the Department of Commerce, the National Science Foundation and the National Aeronautics and Space Administration, and probably represents one of the better examples of inter-agency cooperation within the U. S. Government.

2. Space Environment Forecasting at SEL-NOAA

For the past eight years, the NOAA Space Environment Services Center, (SESC), Boulder, Colorado, has been issuing forecasts of selected variables related to disturbances of the space environment. A summary of the general aspects of the forecasting program of the SESC comprises the following:

a. A network of solar observatories which continuously monitor (visually, film and strip chart record) the solar disk and a periodically report significant solar activity to the central forecast center.

b. Regular reports to the central forecast center from satellites in near earth orbit and irregular reports from satellites in solar orbit. These provide data concerning solar activity levels (x-rays, particle fields, magnetic fields, solar wind).

c. Continuous evaluation of these reports at the central forecast center for the purposes of

   1. Data interchange
   2. Forecast preparation to agencies concerned
   3. Alerting

d. A weekly publication which summarizes solar geophysical data collected in the previous seven days.

These general aspects are more fully defined in the following tables:

Table II

Global Network of Solar Observing Sites

	Equipment	Operated by	Hours of Operation
Athens	*Optical telescope **Radio telescope	AWS	0400Z-1600Z
Puerto Rico	*Optical telescope	AWS	0900Z-2100Z
Sagamore Hill	**Radio telescope	AWS	0900Z-2100Z
Boulder	*Optical telescope ***Radio telescope Sweep frequency Magnetometer	NOAA	1100Z-2300Z
Hawaii	*Optical telescope	AWS	1500Z-0300Z
Carnavon	*Optical telescope **Radio telescope	NOAA/NASA	2300Z-1100Z
Tehran	*Optical telescope	AWS	0200Z-1400Z

*Optical telescope -Hα and white light
**Radio telescope -Discrete frequency (245, 410, 606, 1455, 2700, 5000, 8800 MHZ)

***Radio telescope -Discrete frequency (245, 1495, 2700, 5000 MHZ)

Table III

Satellite Reports to the SESC

Satellite	Sensors	Coverage/Delay in receipt of data
SOLRAD HI	x-rays	60%/1 to 2 hour delay
NOAA 4	particles	Continuous/3 hour delay
DSP	particles	Continuous/1 hour delay
PIONEER	particles solar wind magnetic flux	< 5% coverage/∿2 hour delay
GOES-1 and SMS-2	particles magnetic flux x-rays	Continuous/0 delay

Central Forecast Center

Boulder, Colorado - 24 hr/day operation. Manned by AWS (Air Weather Service) and NOAA professional "solar forecasters." Forecasts are issued twice daily and disseminated to approximately 60 agencies. These forecasts provide existing and predicted (next 3 days) information concerning solar geophysical conditions (solar activity, flares, solar radio flux,and geomagnetic conditions).

In addition, warnings (or alerts) are issued to approximately 100 agencies whenever a solar geophysical event of concern to these agencies occurs or is imminent.

Once daily a special forecast is provided to the SST program. These SST forecasts are derived from -

a. Solar activity levels (recent past, current and imminent)

b. Polar riometer responses (current)

c. Proton sensor response (current and recent past)

More precise SST forecasts are provided by a regular PILOT REPORTING system whereby current radiation levels in Polar regions (SST altitudes) are routinely provided SESC. This data input was established with the launch of the solar proton monitor aboard the synchronous Meteorological Satellite SMS-1 in early 1974. The detectors on the current GOES-1 and SMS-2 satellites monitor solar protons to energies of 500 MeV with real time data transmission to the SESC.

A reprint containing a description of the Solar-Terrestrial Monitoring system will be found to accompany this report.

VERIFICATION OF SPACE ENVIRONMENT SERVICES CENTER FORECASTS

1. Introduction

The Space Environment Services Center (SESC) issues forecasts of selected geophysical variables every six hours and the discussion here refers to the forecasts issued at 1800 UT. Two different types of forecasts are issued: those stated in probabilistic terms, which are used for flares and proton events; and those of anticipated magnitude, which are issued for values of 10-cm flux and planetary magnetic index Ap. This document will consider only class M and X flares and proton events, although a third class (C) exists. The flare classification is determined by the emitted X-ray flux between 2 Å and 8 Å with:

Class C: $.001\ erg/cm^2 sec < flux < .01\ erg/cm^2 sec$

Class M: $.01\ erg/cm^2 sec < flux < .1\ erg/cm^2 sec$

Class X: $flux > .1\ erg/cm^2 sec$

While the interest of the reader of this document rests primarily with proton events, consideration of the forecasts of major flares and their verification is also of concern for two reasons. Solar proton events are sufficiently rare that the statistics of the verification scheme leave something to be desired, and secondly, since solar proton events have a flare origin, a forecasting scheme that can not demonstrate "skill" in forecasting flare activity can certainly not convincingly claim skill in forecasting the major events that may produce solar proton events.

The SESC issued forecasts for each element for one, two, and three days in advance. To simplify the verification, the forecasts are listed in all tabulations according to the date to which they applied, rather than to the date on which they were issued.

2. Probability Forecasts

The forecasts issued for flares and proton events are expressed as probability statements. As currently issued, they are basically subjective and are based on a study of the recent history of the activity on the sun. In preparing such probability forecasts, the forecaster is concerned with classifying the current situation into some sort of ordered set and with assigning to the members of the set a numerical value that represents the actual probability that an event of the given type will be observed. Sanders (1963) uses the terms "sorting" and "labeling" to describe these two aspects of the problem. It is possible to assess the forecaster's success in sorting by seeing if the days to which he assigns higher probabilities actually are those on which higher proportions of events are observed, whether or not the precise numerical values agree. This can be done by grouping the days according to one of several ranges of forecast issued for that day and examining the proportion of events observed in each of the several groups. In this study, the forecasts have been grouped into quartiles, the observed proportion of events and 95-percent confidence interval have been calculated for each quartile, and the values have been tabulated and plotted to facilitate their use. Skill in sorting will be reflected by an increase in the observed proportion of events as the stated probability of the event increase.

The graphs for Class M flares indicate that the forecasters have considerable skill in sorting for these events. Even in Class X flare and proton event forecasts this skill is evident to some degree, although the much smaller number of cases that fell in the greater than 25-percent probability categories tends to mask this result. It is quite apparent from these same graphs that the forecasters have demonstrated little skill in labeling their forecasts with actual probabilities. There was a persistent tendency to over-forecast, which is particularly obvious for the Class M (or greater) events. Thus a higher forecast probability indicated, in general, a higher true probability, but the true probability did not rise anywhere nearly as fast as the forecast.

Many different sorting methods have been proposed for measuring the overall effectiveness of probability forecasts. Unfortunately, "effectiveness" is an elusive quantity and should be measured differently, depending on user needs. Where these needs cover a wide range, the Brier P-score (Brier, 1950) gives a good general measure, but is best used for comparing two alternative forecast schemes. Sanders (1963) recommended that the P-score of the actual forecasts be compared with the P-score for a constant forecast based on the climatology of the events. The users of flare forecasts, however, have less broad needs. Most of them appear to be concerned more with the missed event than with false alarms, and the forecasters indicate that they tend to tailor their forecasts to meet the requirements of this group of users. Despite this limitation, the P-scores have been compared as suggested above, with the climatological forecast defined to be the proportion of events observed during the quarter year immediately preceding the verification period. Based on the criteria suggested by Sanders (1963), only the Class I flare forecasts are as effective as the climatologically based constant forecast. It should be borne in mind that the P-score, which is essentially a mean square error of the probability forecasts, combines contributions from two types of errors: one caused by the difference between the mean of the forecasts and the observed proportion of events (a labeling factor), and the other caused by incorrectly classifying a situation into a greater than (or less than) normal expectancy category (a sorting factor). As we have already observed, the labeling errors are large and probably dominate the P-scores.

One problem encountered in the verification of the proton-event forecasts and, to a much lesser degree, of the flare forecasts is the difficulty in objectively defining what constitutes an event. If we are to define an event-day as one on which proton flux values are high, it becomes a trivial exercise to issue forecasts with impressive scores because of the persistence of such events. We have adopted a definition of a proton event as one that results in a significant increase in the proton flux as determined by terrestrial sensor (specifically an absorption increase of 1 dB on a 30-MHz riometer located in the polar cap -- this is inferred to represent a flux of approximately 16 protons cm^{-2} sec^{-1} $ster^{-1}$ with energies greater than 14 MeV). For 1972, only three such events were observed. There is some tendency for the forecasters to keep the forecast probabilities high after an event to indicate that the flux of protons will still be high. Because of the strict definition of an event, this tendency results in degradation of the score.

Summary statistical verification data on Class M, Class X, and proton event forecasts are shown in the following pages for year 1972.

Computer generated Figures 5, 6, 7, and 8 indicate the one day probability forecasts for the labeled events, and the vertical dashed lines denote the actual occurrences of these events through 1972, while Figure 9 constitutes plots of the observed proportion of class M flares versus the one, two and three day forecast probabilities, as indicated.

It will be noted that the correspondence between the observed and predicted proportions lie reasonably close to the dashed 45° line, which would be obtained from perfect forecasts.

SESC FORECAST VERIFICATION

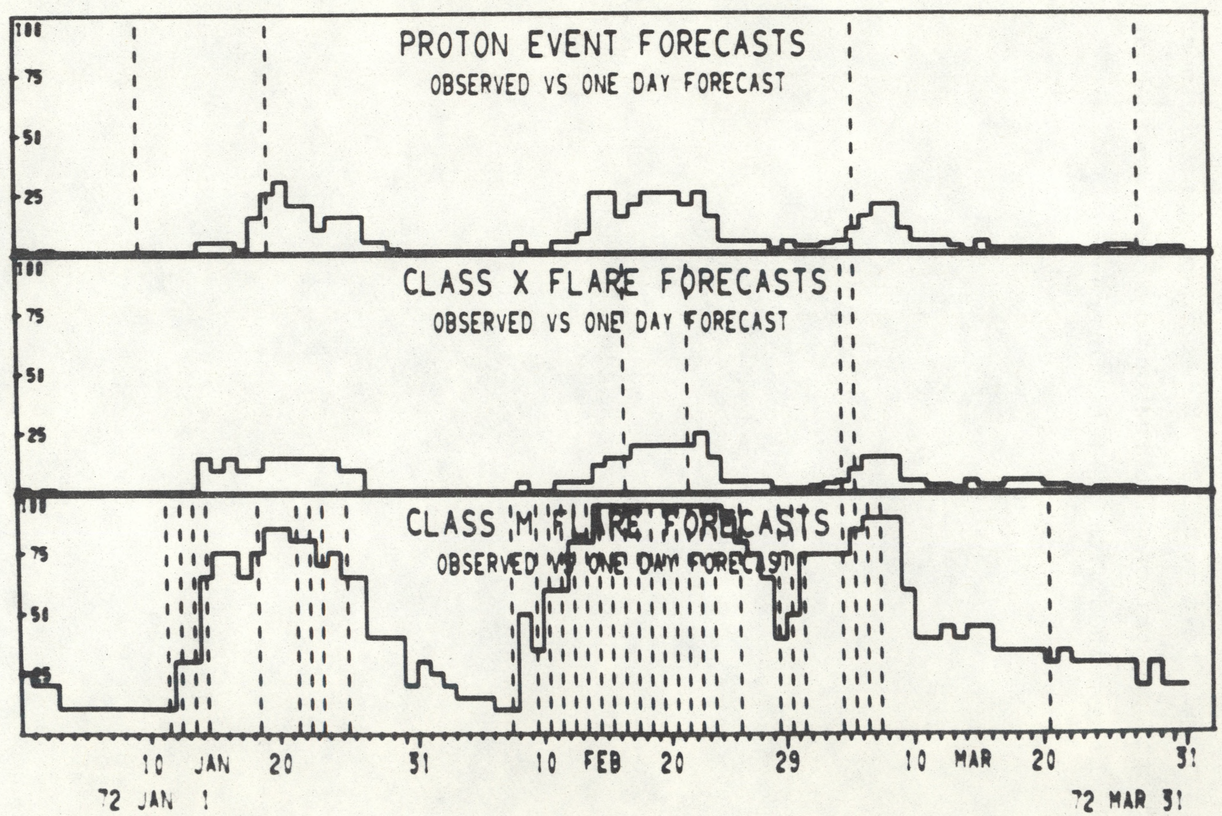

Figure 5

SESC FORECAST VERIFICATION

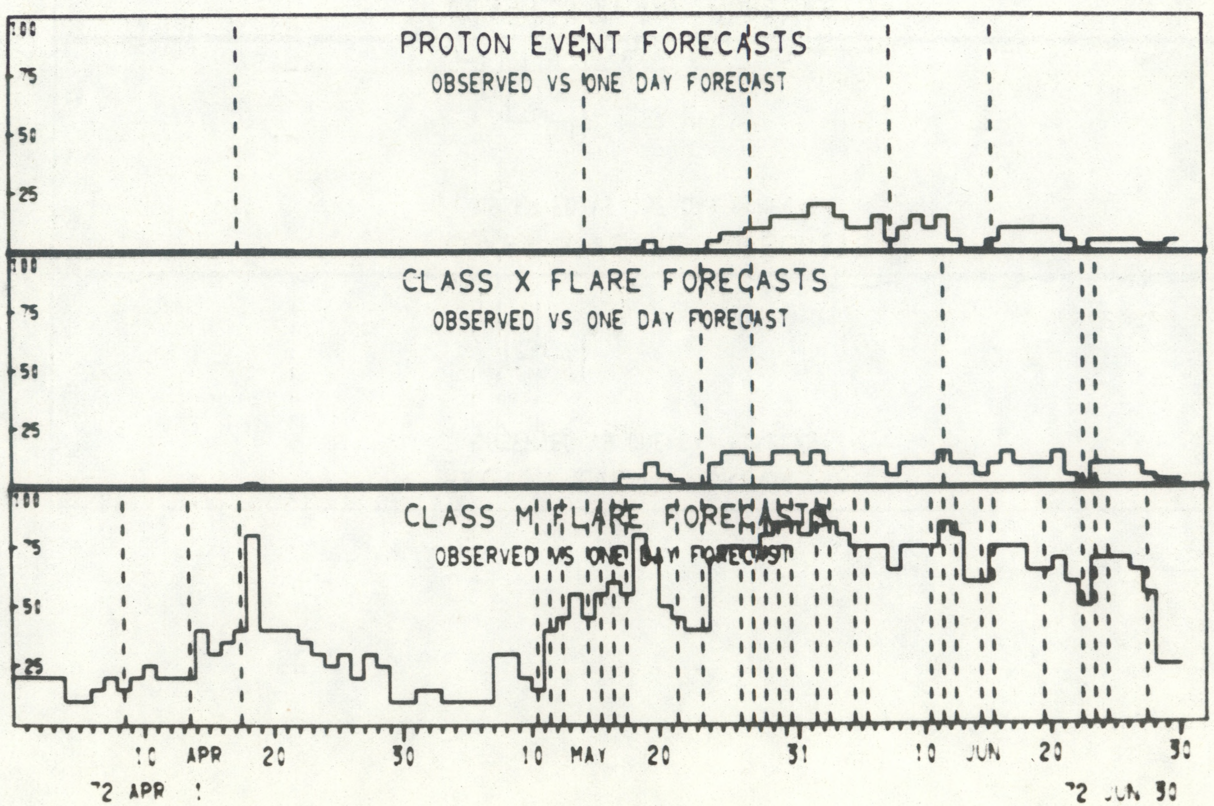

Figure 6

SESC FORECAST VERIFICATION

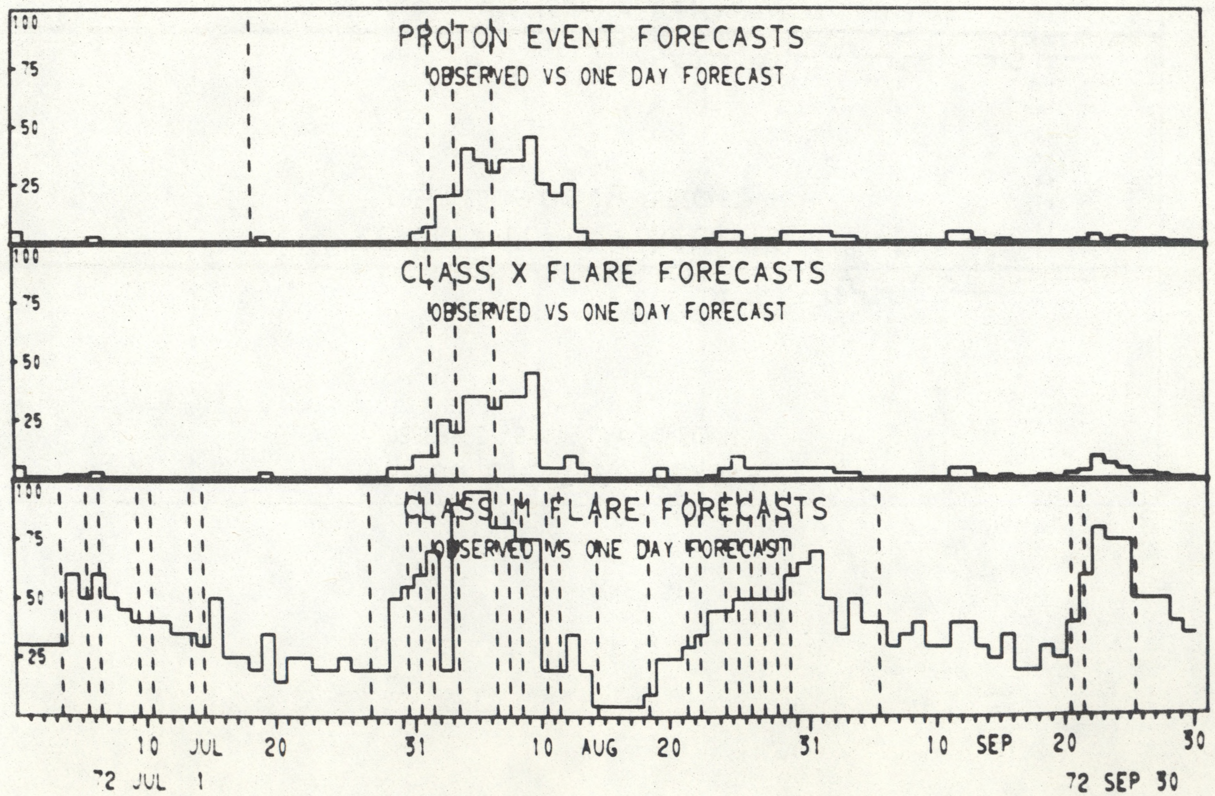

Figure 7

SESC FORECAST VERIFICATION

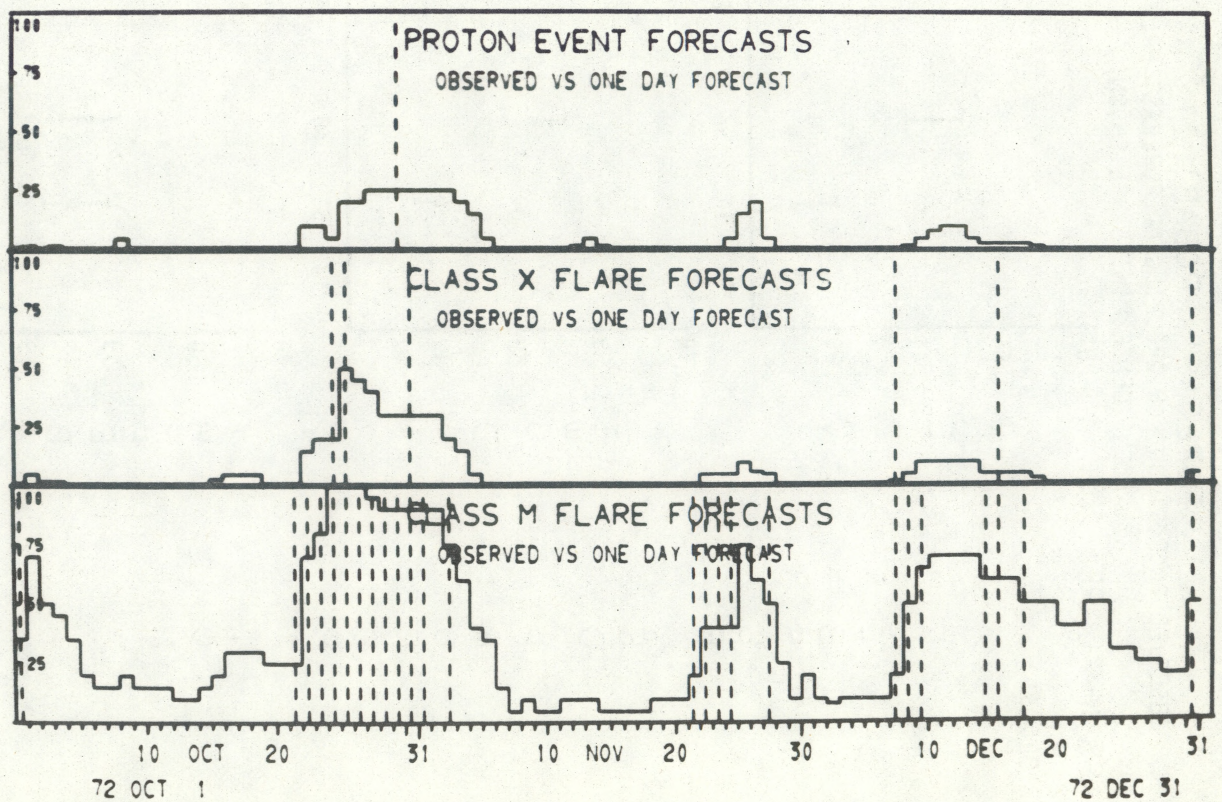

Figure 8

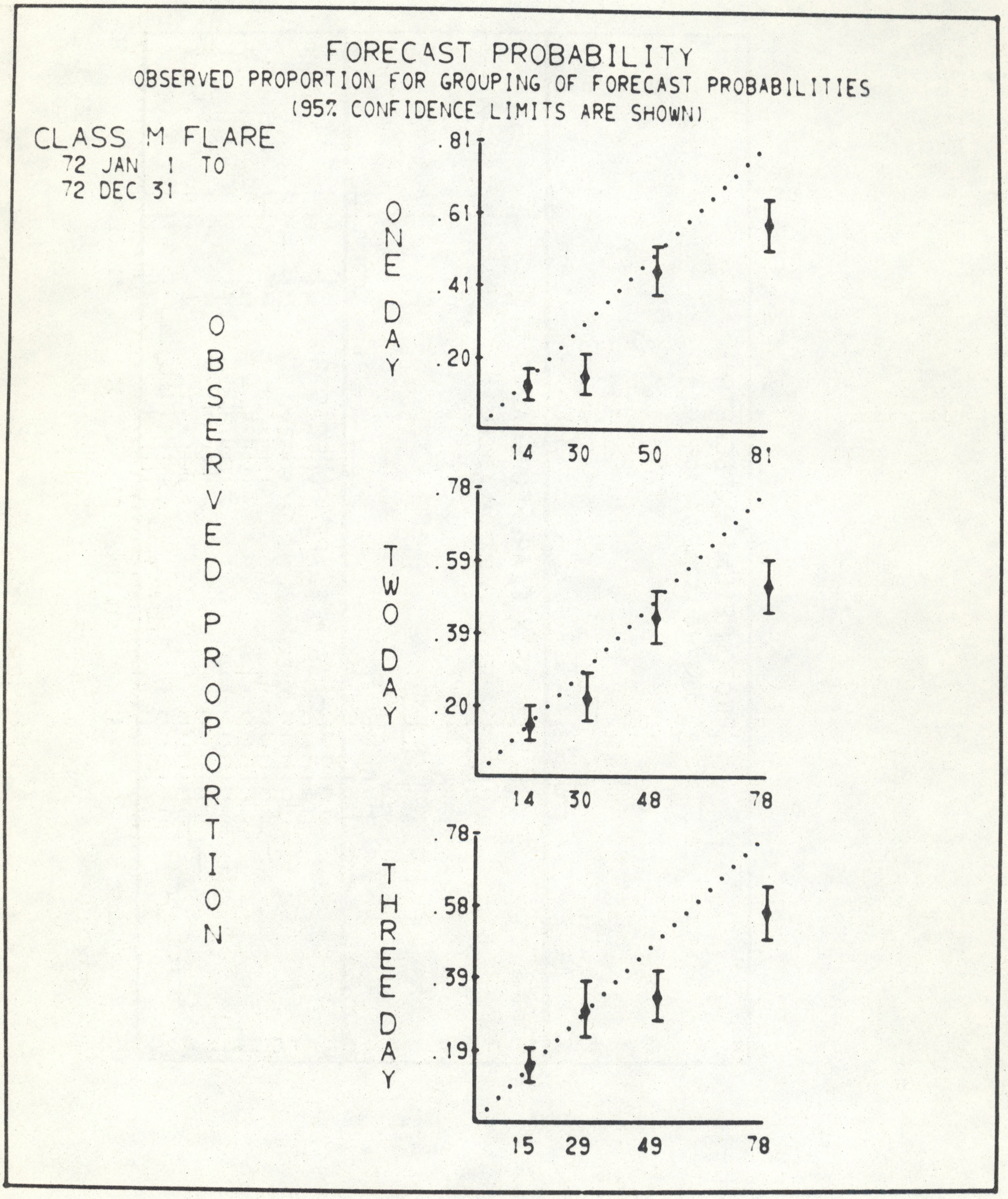
FORECAST PROBABILITY
OBSERVED PROPORTION FOR GROUPING OF FORECAST PROBABILITIES
(95% CONFIDENCE LIMITS ARE SHOWN)
CLASS M FLARE
72 JAN 1 TO
72 DEC 31
OBSERVED PROPORTION
ONE DAY
.81
.61
.41
.20
14 30 50 81
TWO DAY
.78
.59
.39
.20
14 30 48 78
THREE DAY
.78
.58
.39
.19
15 29 49 78

Figure 9

PROTON EVENT FORECAST AND WARNING

1. Introduction

Since February 1969 daily radiation forecasts (SOLTERWARN) have been issued to the Royal Aircraft Establishment in support of the Concorede program. The Solterwarn forecasts are issued at 2200-2300 UT and are in two parts. The first part gives an estimate of the current value of the radiation doserate equivilent at an altitude range of 50,000 to 60,000 feet, and at 50^{O}N geomagnetic latitude in terms of a color-code range:

Green = < 10 mrem/hr.

Amber = 10 - 100 mrem/hr.

Red = < 100 mrem/hr.

The 100 mrem/hr. level is currently anticipated as the level at which action (i.e. altitude reduction) is required. The second part of the Solterwarn gives the confidence factor of a forecast that Amber or Red conditions will be experienced on the next and following two days. A low confidence that an Amber condition will be experienced implies a high confidence that a green condition will exist.

This discussion will briefly outline the means by which dose rates are currently estimated, and will evaluate the Solterwarn forecasts given for the past two years.

2. Estimation of Dose Rates

Dose Rates are currently estimated both from deduction of approximate proton spectral characteristics from ground based riometer observations and from extropolation of satellite determinations of proton flux to higher energies.

Estimated geomagnetic cut-off values at a number of riometer observing sites along with a variety of assumed solar proton spectra have been used to develop a family of graphs. Once determined, these graphs are used in combination with observed riometer absorption values to estimate the actual solar proton spectra at the top of the atmosphere. Dose rates reduced from these spectra are then estimated from the curves of Flamm and Lingenfetter (1964). The riometer results are based on the H (P, Po) values determined by Juday and Adams (1970), but modified for different geomagnetic cut-off values.

Some reservations should be considered in the use of such riometer observations in the deduction of spectra, and ultimately, dose rates at attitude:

1. All of the curves are dependent on station geomagnetic cut-off values. Even during quiet times these are not precisely known. Thus, during quiet conditions, P_o, J_o values obtained from these graphs are somewhat crude (depending on which estimates are used for quiet cut-offs and D-region coefficients, J_o values can vary by a factor of almost 10 for a given event.)

2. During magnetic storms, cut-off values are reduced, generally by an unknown amount. The curves, computed for quiet time, cannot be applied during disturbed conditions. (One type of situation exists in which certain curves can be used. This case will be described later.)

3. Nighttime riometer responses are known to be drastically reduced relative to daytime values; further it appears that:

   a. initial states of proton events are just not observed by riometers at night and

   b. during later nighttime stages, when some absorption may be apparent, the required theory is far too shaky to permit establishing proton fluxes from the absorption.

4. Juday and Adams state that, for their method, the assumption of a single exponential rigidity spectrum to describe the protons is not critical; their method does not employ a chain of stations with different cut-offs to get P_o, but rather works always with flux above zero cut-off. Our approach, however, will require cutting off the spectrum at differnt rigidities; the above cut-off-spectra may be quite different from one station to the next. We retain the assumption of a single "effective" spectral form, acknowledging that this may be uncertain, especially for station cut-off $\sim$ 100 MV.

Because of the uncertainties mentioned before of deducing spectral parameters from riometer observations, it is clear that direct satellite measurement of proton fluxes are more desirable in determining the spectra. Until 1976, however, the highest instrumental thresholds of the detection carried by the TIROS operational satellite, and by ATS-1 were about 60 MeV, approximately that minimum energy required by protons to reach and affect the altitude range of interest to aircraft. It was therefore necessary that the spectral parameters be determined over a lower, and therefore less appropriate range. This deficiency was significantly reduced with the launch of the Synchronous Meteorological Satellite GOES in early 1974.

The solar proton monitor aboard GOES extends the integral flux measurements to protons of > 500 MeV, and allows significantly improved estimates of the spectral parameters for radiation hazard assessment. The observations from the GOES Monitor are available continuously to the SESC in real-time and permit continual and relatively accurate deduction of solar proton spectra over energy ranges of importance.

The Use of Two or More Riometer Responses to Determine P_o and J_o

Throughout this study, the exponential rigidity form of solar proton spectrum is used.

$$J(>P) = J_o e^{-P/P_o}, \tag{2}$$

where J_o is the total proton flux above zero rigidity or energy; P_o is the e-folding rigidity - a parameter describing the hardness of the spectrum; and $J(>P)$ is the integral flux above rigidity P. At any given station that station's cut-off value determines the low rigidity limit for entering particles; thus the value of P in the equation is the station's rigidity cut-off.

Consider two riometer stations with estimated cut-offs P_1 and P_2.

$$\frac{J(>P_1)}{J(>P_2)} = \frac{J_o e^{-P_1/P_o}}{J_o e^{-P_2/P_o}}. \tag{3}$$

By dividing one flux value by the other, J_o is eliminated and the only spectral parameter remaining is P_o.

Juday and Adams give a group of $H(P,P_o)$ graphs; the H-parameter is defined as

$$H(P,P_o) = \frac{J(>P)}{A^2}, \tag{4}$$

where A is the riometer absorption for a zero cut-off station. We modified these H values to apply when the absorption corresponded to various non-zero station cut-offs, P_x.

Substituting we get

$$\frac{H(P_1,P_o)A_1^2}{H(P_2,P_o)A_2^2} = \frac{e^{-P_1/P_o}}{e^{-P_2P_o}} . \quad (5)$$

Substituting in a variety of assumed hypothetical P_o values and the corresponding H values for each station cut-off, we calculate ratios of

$$\frac{A_1^2}{A_2^2}, \text{ and } \frac{A_1}{A_2} \quad (6)$$

By this means, the curves of figures 10 through 14 are constructed. Similarly, figures through are obtained by substituting in a variety of assumed P_o and J_o values, for different station P values, in the expression

$$H(P,P_o)A^2 = J_o e^{-P/P_o} . \quad (7)$$

When the curves have been obtained as described, the converse procedure is then used for finding actual values of P_o and J_o from observed absorption values. This procedure will be described.

We have worked with four different riometer stations.

Bar I: $P_{Bar\ I}$ cut-off is taken as 138 MV (E = 11 MeV). This value is higher than the geomagnetic ridigity cut-off at this station. However, protons below this rigidity do not contribute strongly to riometer, or forward-scatter, absorption values, so 11 MeV may be considered an "effective" zero cut-off. Juday and Adams give an H-parameter curve for 11 MeV.

College: P_{Coll} is taken as 190 MV (E = 20 MeV).

Paxson: P_{Pax} is taken as 310 MV (E = 50 MeV).

Sheep Mtn: P_{SM} is taken as 450 MV (E = 100 MeV).

Suppose a proton event has occurred. Select stations whose observed absorption values give an $\frac{A_1}{A_J}$ ratio that is significantly less than 1 (where $P_J < P_1$) and whose A values are both reasonably large, but not > 8db. For a given event, fulfilling all of these requirements may not be possible, and a compromise will be necessary. Having selected the best two stations, use the appropriate figure (between 10 and 14). From the observed absorption ratio, use the curve to read off the value of P_o; then use the absorption value of one of the stations and the corresponding curve (figure between 15 and 18) to read off the value of J_o.

Having now obtained both P_o and J_o, we make use of figure 19. From this, we can read off directly the total dose value, at 65,000 feet, in rem/hour and rads/hour. Note that the curve is normalized to J_o/P_o = 1 proton $(cm^2 sec\ ster\ MV)^{-1}$. The dose obtained from the curve must be multiplied by the actual value of J_o/P_o; note also that the values we have obtained for J_o from figures 15 to 19 must be multiplied by 2π to be used with the dose rate curves.

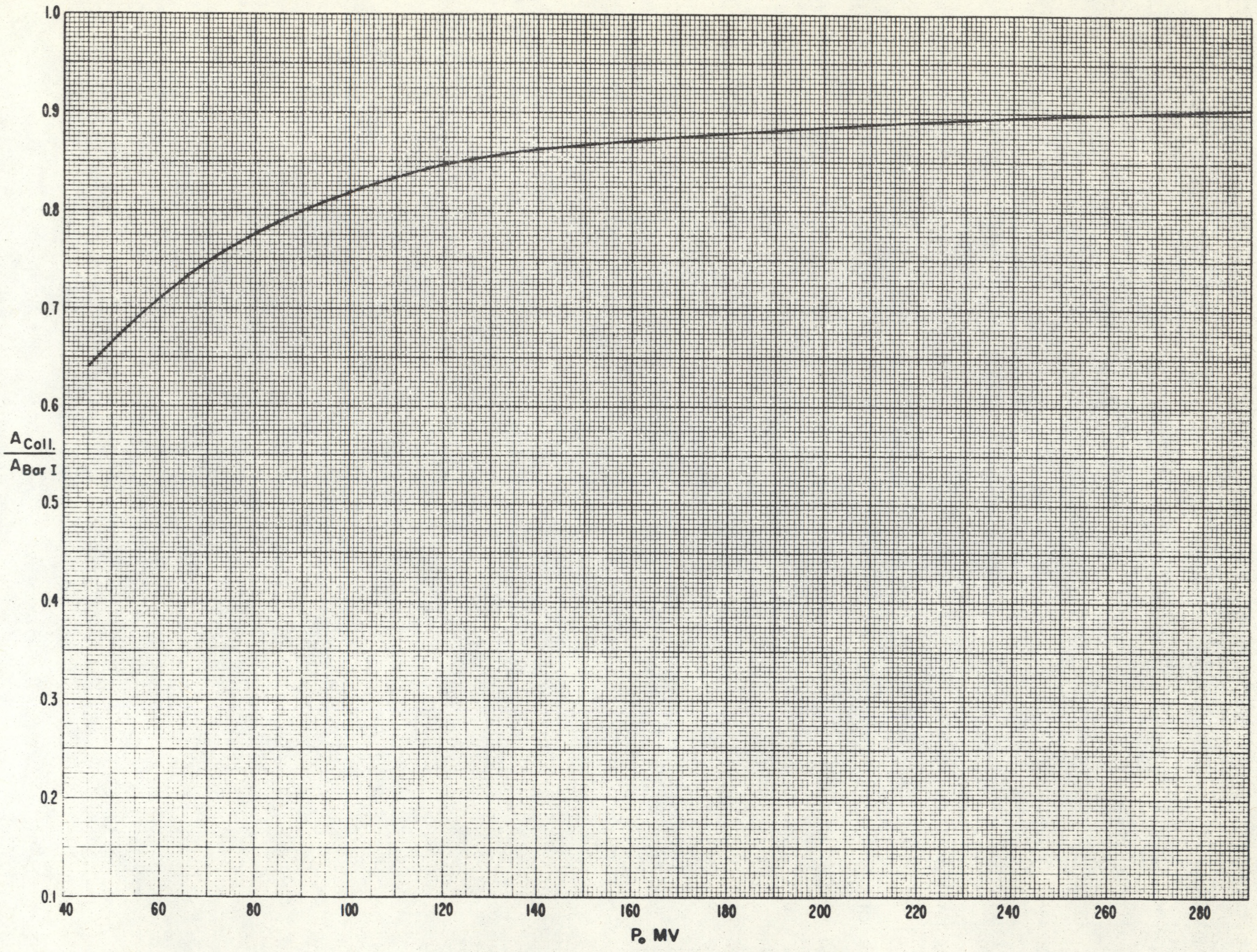

30 MHz Absorption Ratio

Characteristic Rigidity

Figure 10

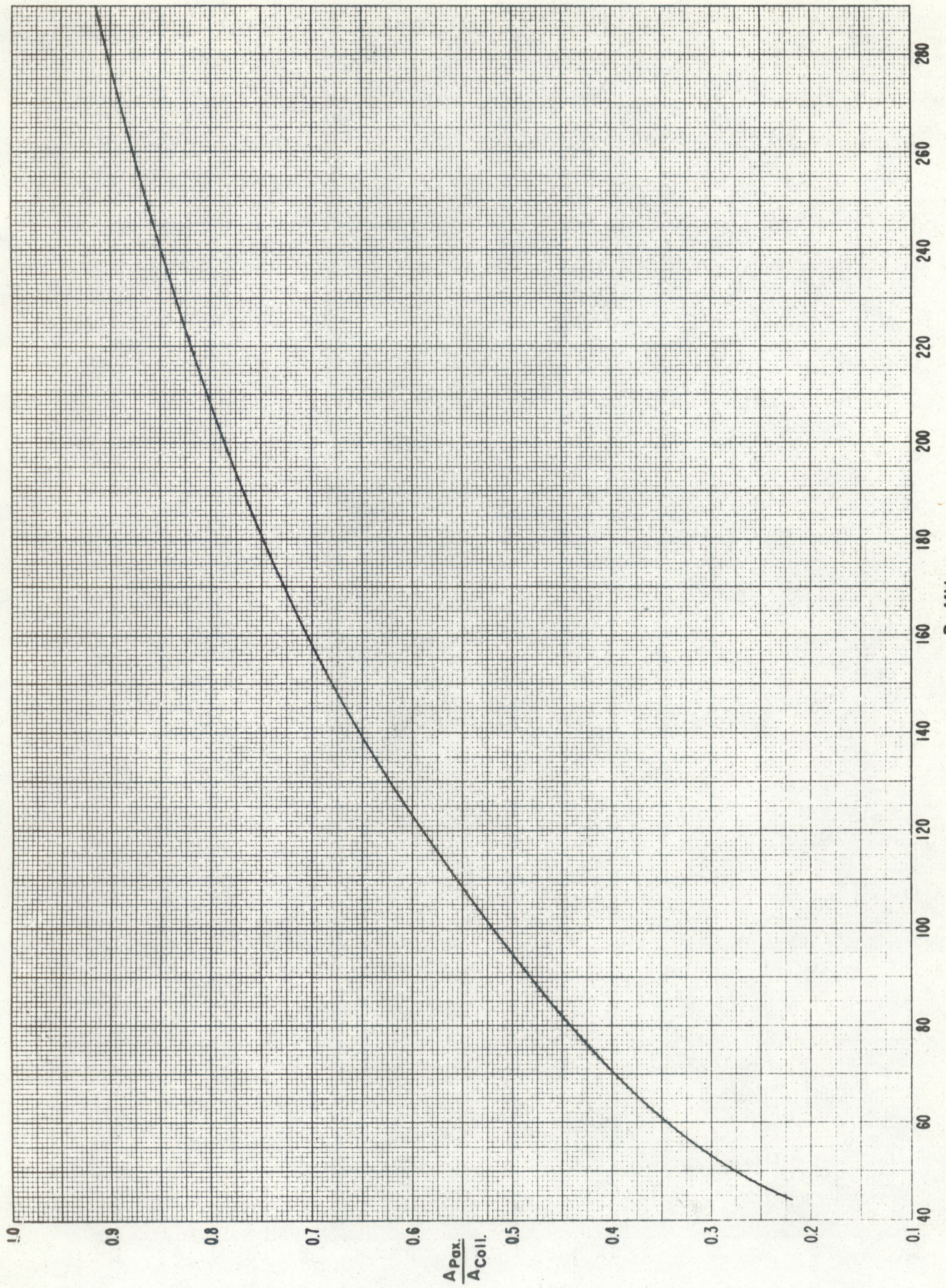

30 MHz Absorption Ratio

Characteristic Rigidity

Figure 11

30 MHz Absorption Ratio

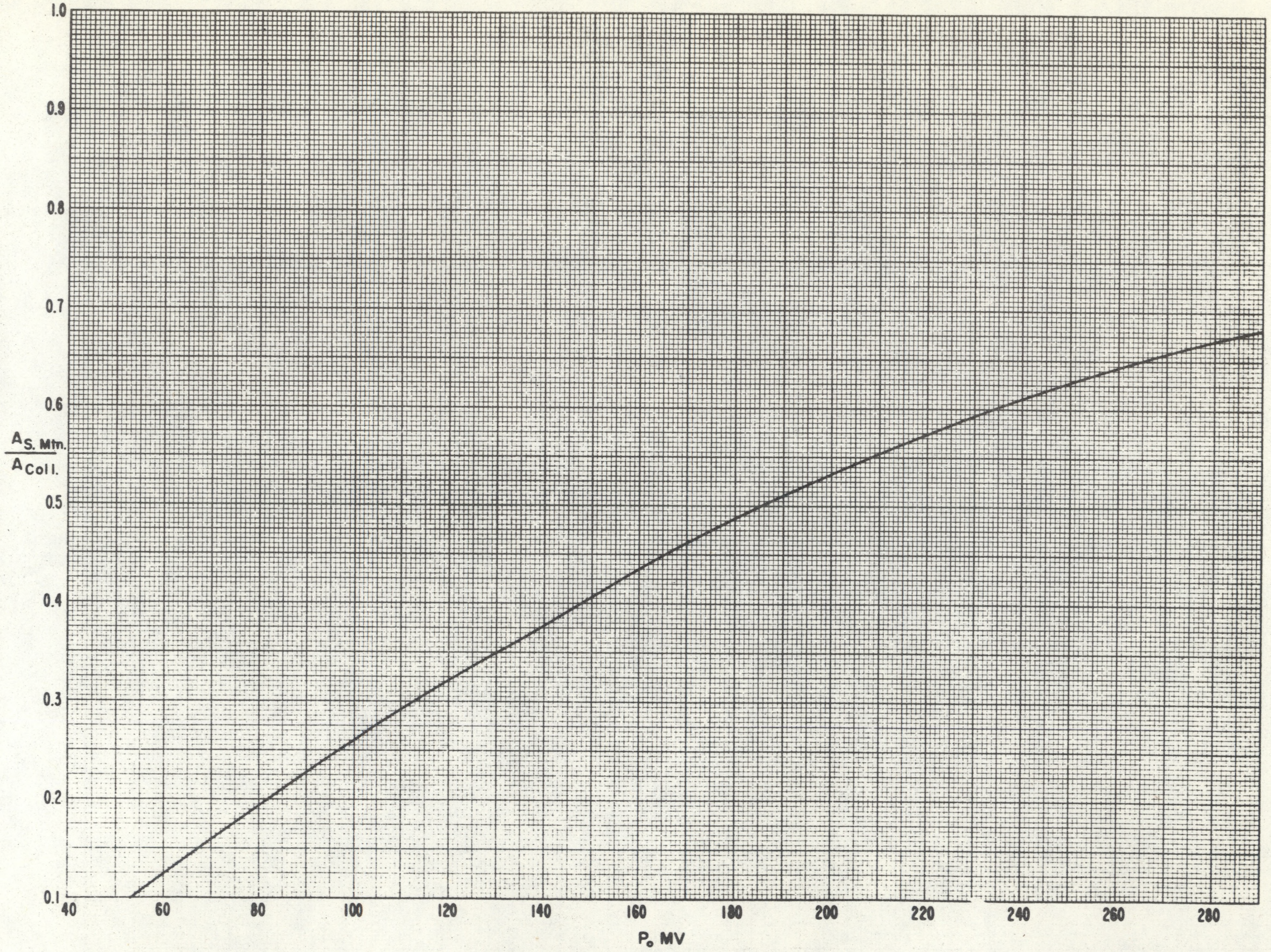

Characteristic Rigidity

Figure 12

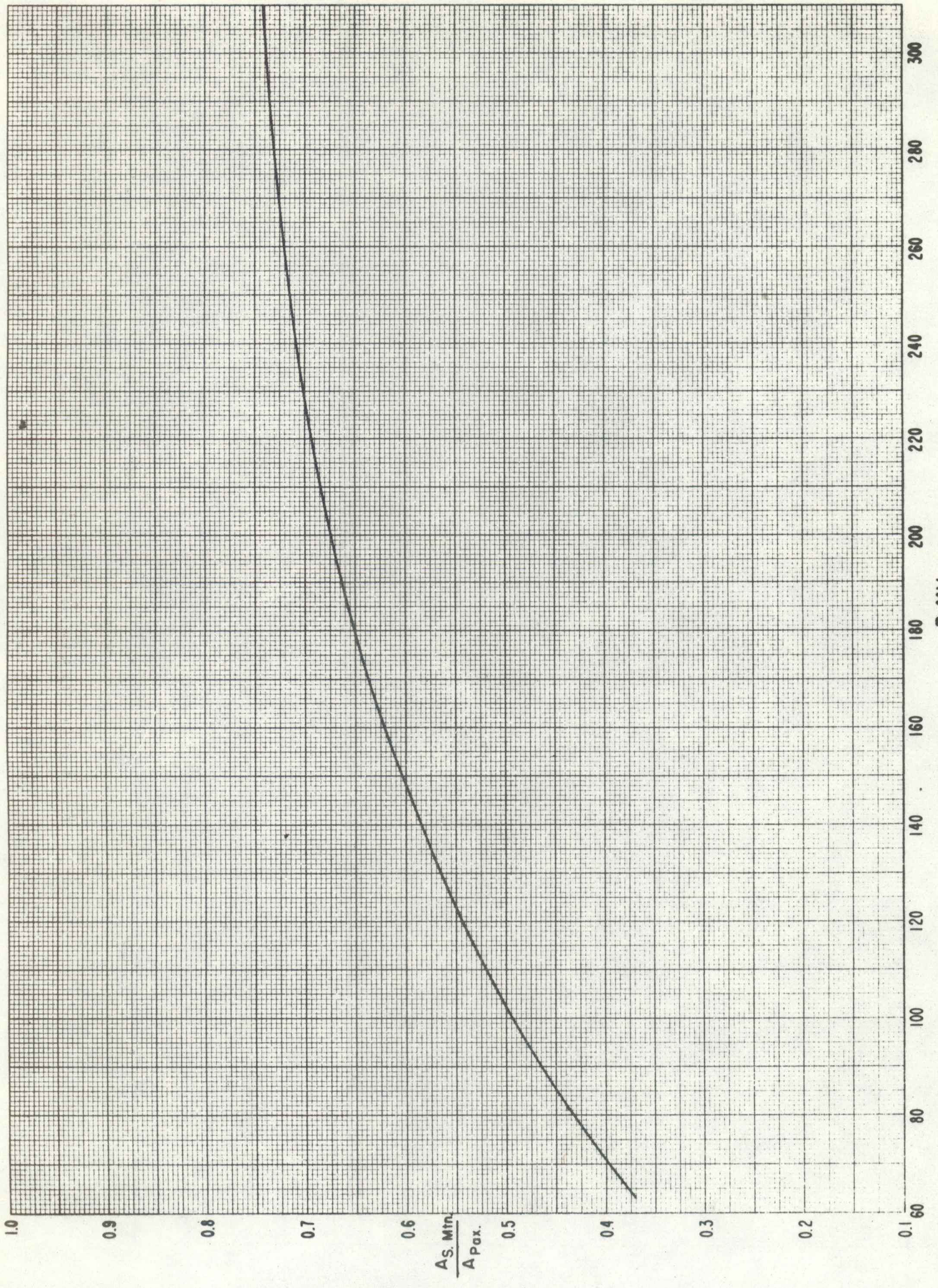

Characteristic Rigidity

Figure 13

30 MHz Absorption Ratio

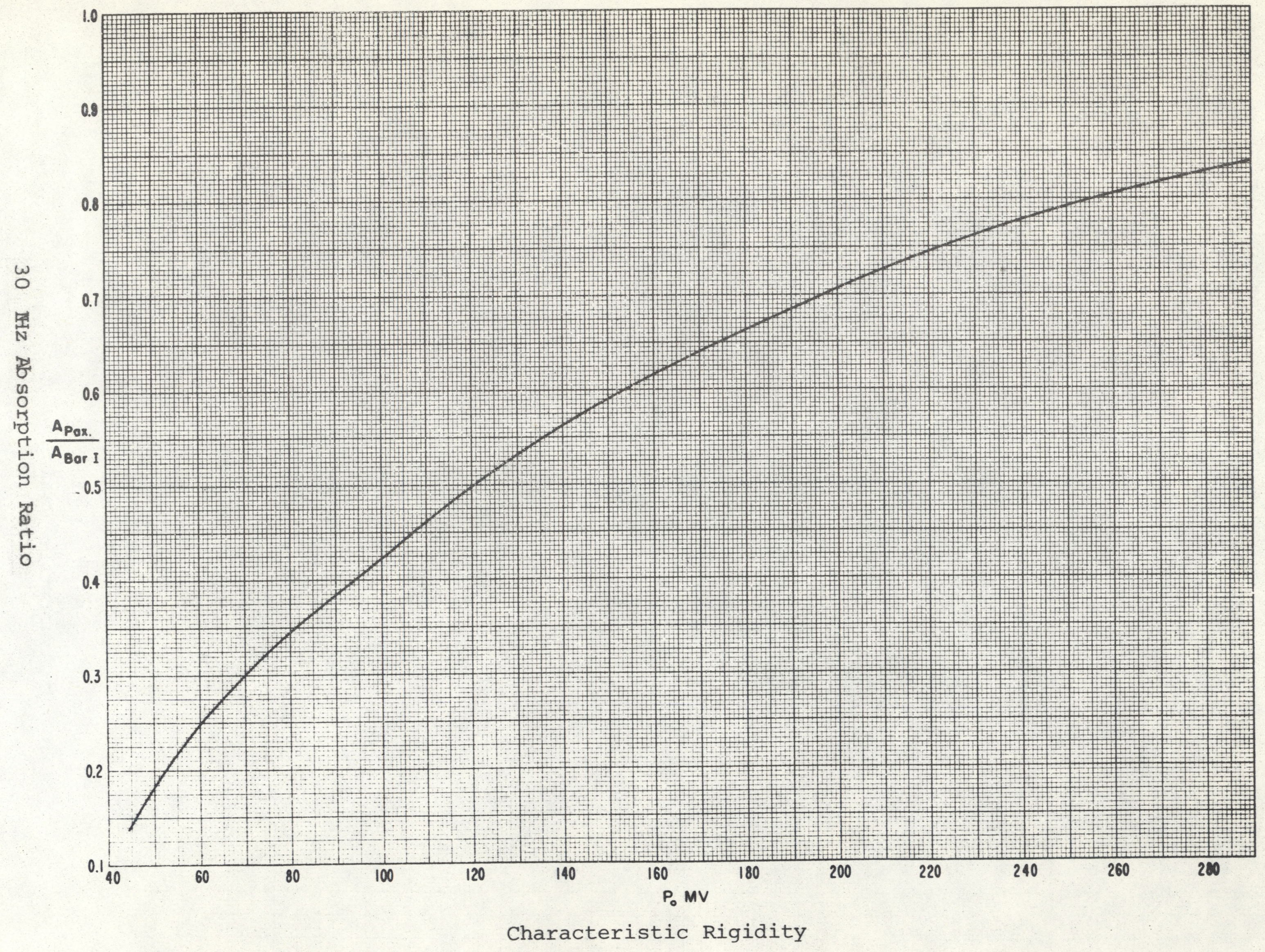
1.0
0.9
0.8
0.7
0.6
0.5
0.4
0.3
0.2
0.1
$\frac{A_{Pax.}}{A_{Bar\ I}}$
30 MHz Absorption Ratio
40
60
80
100
120
140
160
180
200
220
240
260
280
P_o MV
Characteristic Rigidity

Figure 14

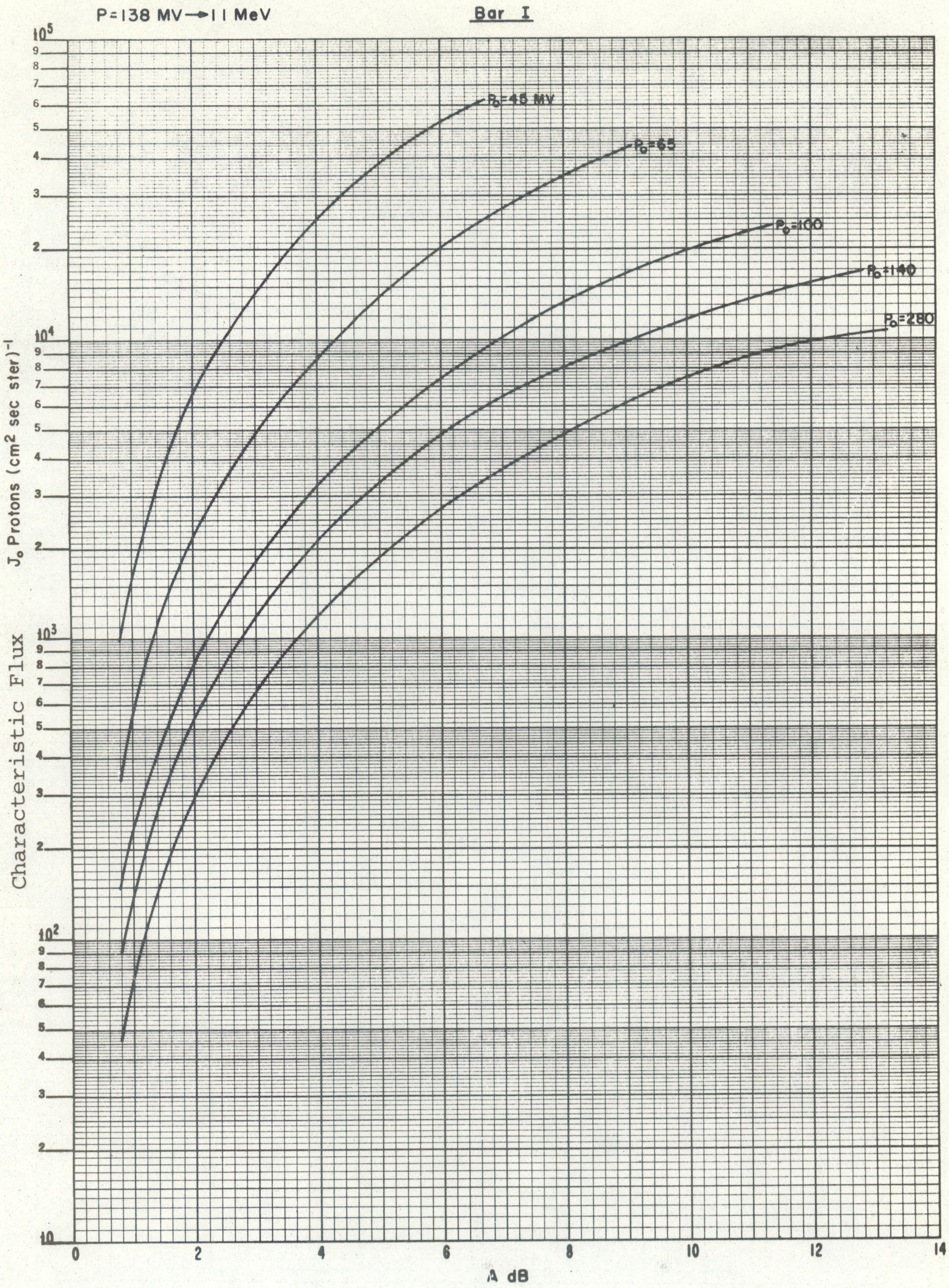
P=138 MV→11 MeV
Bar I
P_o=45 MV
P_o=65
P_o=100
P_o=140
P_o=280
J_o Protons (cm² sec ster)⁻¹
Characteristic Flux
A dB

Figure 15

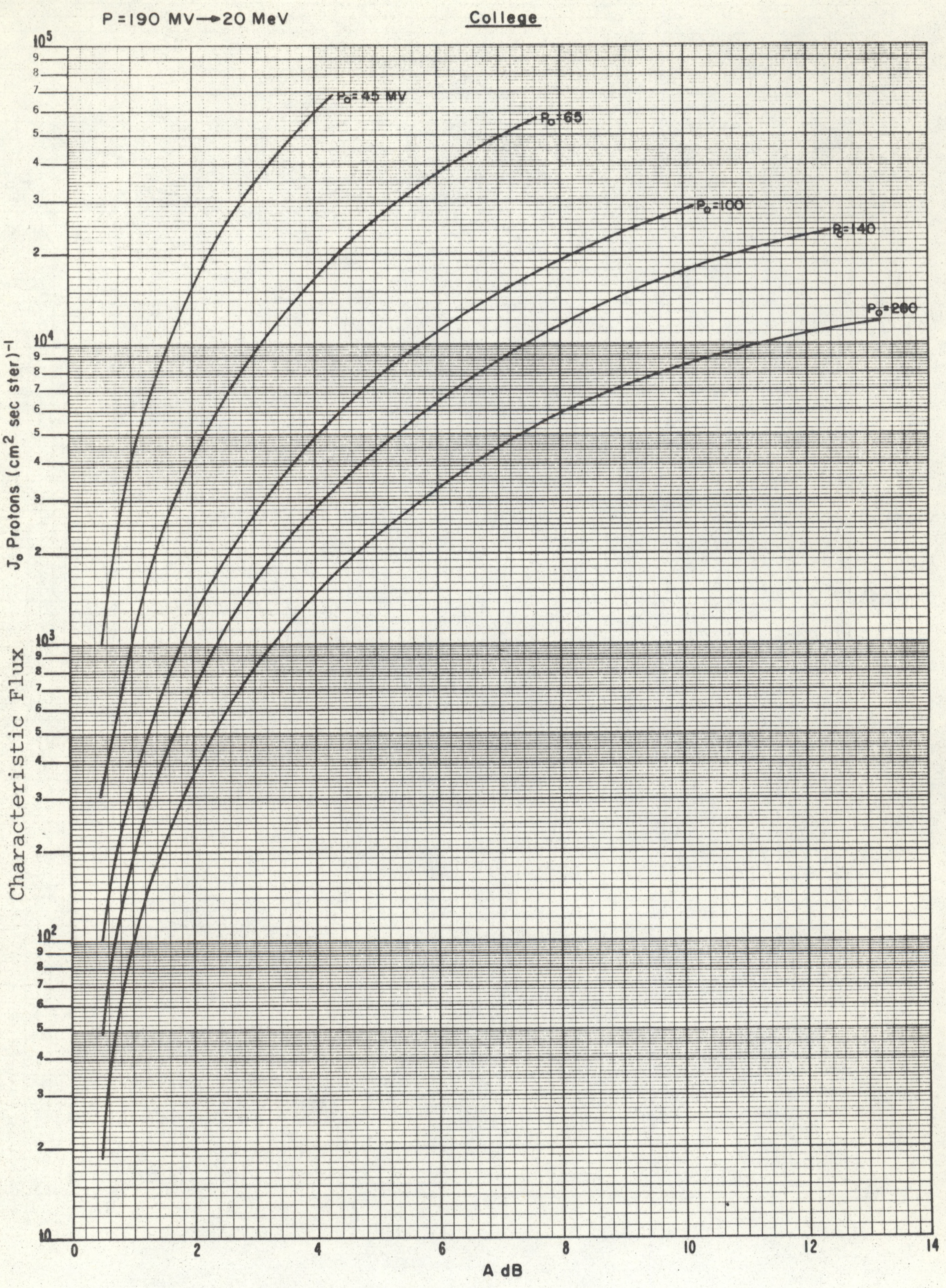
P = 190 MV → 20 MeV
College
P_o = 45 MV
P_o = 65
P_o = 100
P_o = 140
P_o = 200
Characteristic Flux
J_o Protons (cm^2 sec ster)$^{-1}$
A dB

Figure 16

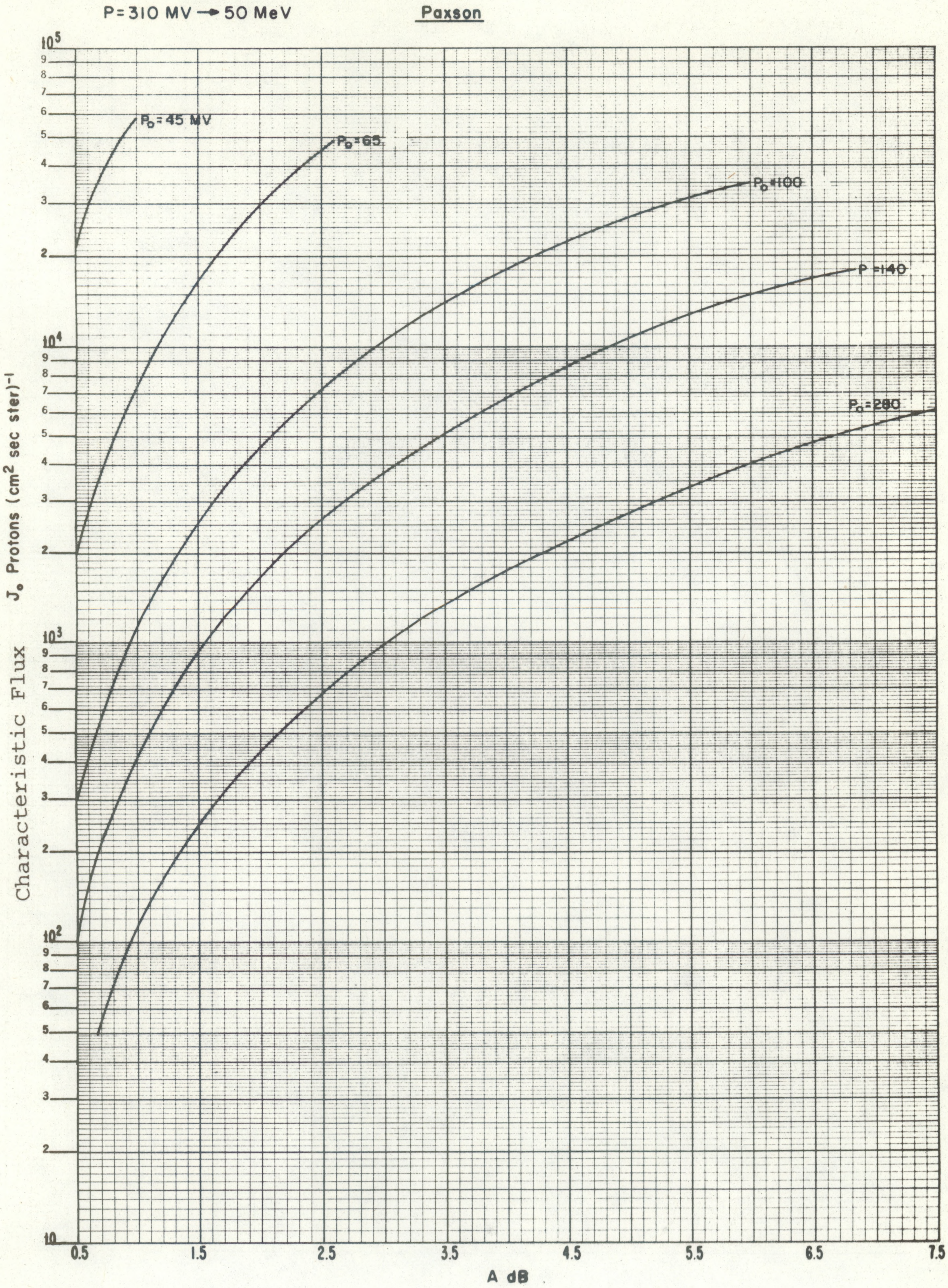

P=310 MV → 50 MeV
Paxson
P_o=45 MV
P_o=65
P_o=100
P =140
P_o=280
Characteristic Flux J_o Protons (cm² sec ster)⁻¹
A dB

Figure 17

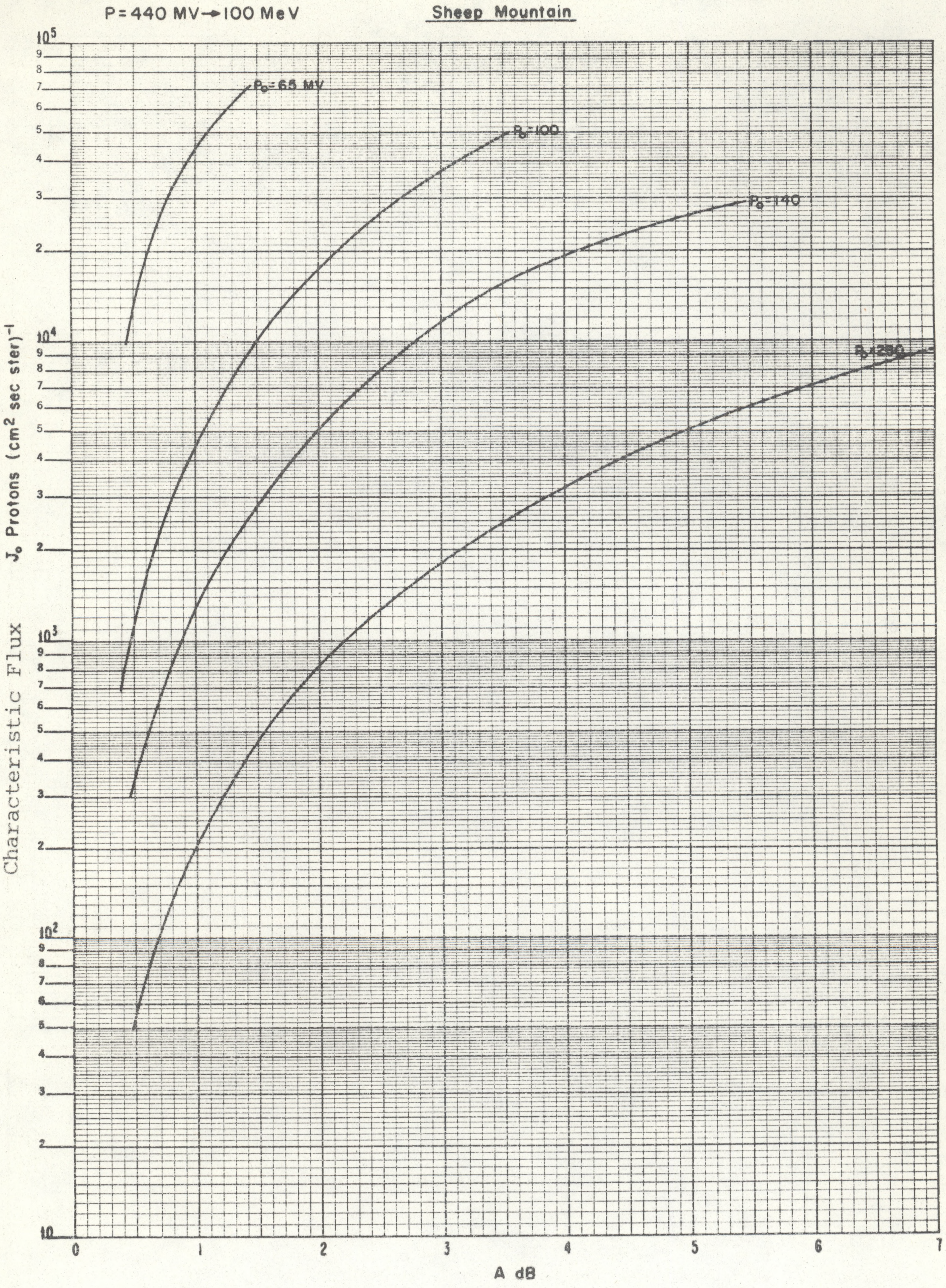

P = 440 MV → 100 MeV
Sheep Mountain
P_o = 65 MV
P_o = 100
P_o = 140
P_o = 280
Characteristic Flux
J_o Protons $(cm^2\ sec\ ster)^{-1}$
A dB

Figure 18

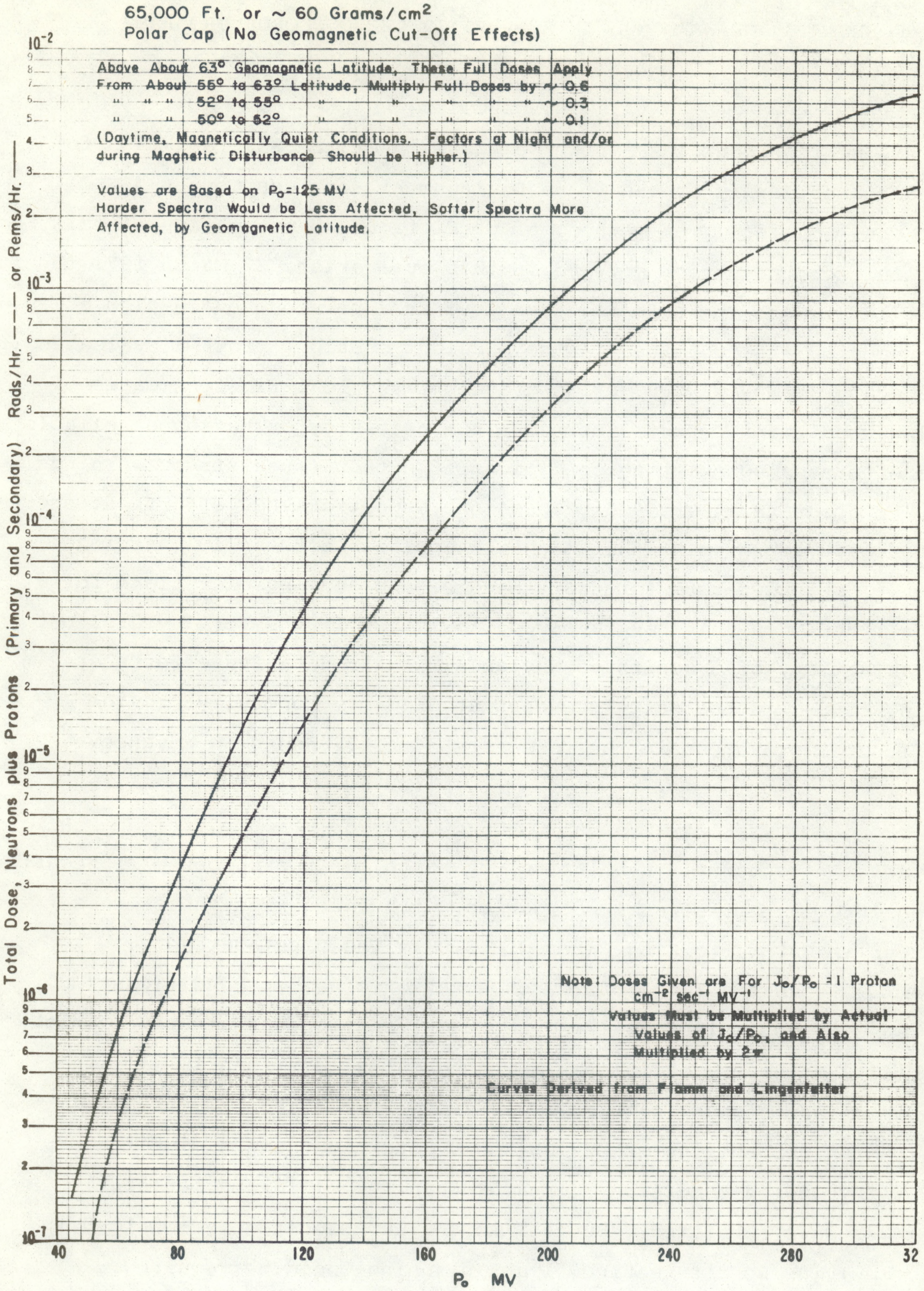
65,000 Ft. or ~ 60 Grams/cm²
Polar Cap (No Geomagnetic Cut-Off Effects)
Above About 63° Geomagnetic Latitude, These Full Doses Apply
From About 55° to 63° Latitude, Multiply Full Doses by ~ 0.6
" " " 52° to 55° " " " " " ~ 0.3
" " " 50° to 52° " " " " " ~ 0.1
(Daytime, Magnetically Quiet Conditions. Factors at Night and/or during Magnetic Disturbance Should be Higher.)
Values are Based on Po=125 MV
Harder Spectra Would be Less Affected, Softer Spectra More Affected, by Geomagnetic Latitude.
Total Dose, Neutrons plus Protons (Primary and Secondary) Rads/Hr. —— or Rems/Hr. ——
Note: Doses Given are For Jo/Po =1 Proton cm⁻² sec⁻¹ MV⁻¹
Values Must be Multiplied by Actual Values of Jo/Po, and Also Multiplied by 2π
Curves Derived from Flamm and Lingenfelter
Po MV
10⁻²
10⁻³
10⁻⁴
10⁻⁵
10⁻⁶
10⁻⁷
40
80
120
160
200
240
280
32

Figure 19

FORECASTS AND WARNINGS IN SUPPORT OF THE CONCORDE PROGRAM

1. INTRODUCTION

This section contains a brief discussion of the SST radiation forecasts as issued daily at the Space Environment Services Center (SESC), Solterwarn, Boulder. The methods of prediction and estimation of existing conditions for the period covered in this evaluation, 22 March 1971 to 29 June 1973, were the same as those used in a previous evaluation of an earlier period and contained in the previous section. Part 2 evaluates the forecast accuracy when verified against the real-time estimates of existing conditions. Part 3 stresses the necessity of having a reliable system of assessing existing conditions if either forecasts or warnings are to be accurate. Part 4 discusses one aspect of SESC efforts at short-term forecast improvement that might be applicable to an SST warning system. The longer-term forecasts have been based on solar flare forecasting techniques that have evolved slowly the last several years, but the availability of a wealth of Skylab ATM solar data and efforts at modeling flares in the next few years at SESC may hopefully provide significant improvement in the forecasts 24 to 72 hours in advance.

2. EVALUATION OF FORECASTS

Table IV contains a tabulation, by month, of the number of forecasts falling into each of several categories, with categories the same as were used in FAUSST Working Paper 8.2.2.08. The first category, 0 to 0.19 amber, covers a range of low expectation of amber conditions (SST dose rates of 10 to 100 millirems per hour) and is equivalent to a high probability of green conditions (SST dose rates less than 10 millirems per hour). The highest category, 0.20 to 0.29 red, represents a relatively high probability of having amber conditions and a significant possibility of red conditions (greater than 100 millirems per hour). Of the 820 days tabulated, 780 fell in the lowest category - 0 to 0.19 amber, implying no alternative flight planning would be required.

TABLE IV

ALL FORECAST DAYS

	Estimated Present Level			Forecast for Next Day							Comments
					Amber				Red		
	Green	Amber	Red	0-.19	.20-.39	.40-.59	.60-1.00	0-0.09	0.10-.19	.20-.29	
1971											
March	10			10							
April	28	2		28				1	1		
May	29	2		21	5	3			1	1	
June	30			30							
July	31			29	2						
August	31			26	5						
Sept.	26	4		27	2	1					
Oct.	31			31							
Nov.	30			30							
Dec.	28			28							3 days missing
1972											
Jan.	31			31							
Feb.	28			28							1 day missing
March	30			30							1 day missing
April	30			30							
May	23	3	2	23		1		2	2		3 days missing
June	28			28							2 days missing
July	31			31							
August	24	4	3	23	3		1			4	
Sept.	30			30							
Oct.	31			29	2						
Nov.	30			27	3						
Dec.	30			30							1 day missing
1973											
Jan.	31			31							
Feb.	28			28	1				1		
March	31			31							
April	30			28							
May	31			31							1 day missing
June	29			29							
TOTALS	800	15	5	780	23	5	1	3	5	5	

Of the 40 remaining days, 13 were forecast as having a significant probability of red conditions. Of these 13, five were actually evaluated as being red in the "existing" tabulation (Table V). These five include all days that were evaluated as red. If a threshold for making alternate flight plans had been set to include just red forecasts, all red days would have been forecast and there would have been eight days of false alarms - a false alarm rate of 62% (Table VI). Repeating a point made in the previously referenced FAUSST paper, although the forecasts were only 38% correct in terms of red days occurring when they were forecast, only 13 days in nearly 27 months (1.6% of all days) would have required alternative planning. To be more conservative, if the threshold were put at 0.60 amber, 14 days are included and the false alarm rate rises to 64%. Finally, if all forecasts higher than 0.40 amber are included, 19 days (2.3% of all days) would have required preparation measures. Fourteen of these would have been false alarms and five still would have been correct forecasts. When verified by real-time "existing" conditions, the forecasts appear to be useful. However, it will be noted in Part 4 that there is room for considerable improvement in the real-time estimation of existing conditions.

TABLE V

ALL 'EXISTING' AMBER OR RED DAYS

		Forecast (Day - 1)		
Date	Existing	Green	Amber	Red
1971				
6 April	Amber		.01	
20 April	Amber		.01	
14 May	Amber		.40	
16 May	Amber		.01	
1 Sept.	Amber		.00	
2 Sept.	Amber		.50	
3 Sept.	Amber		.25	
4 Sept.	Amber		.25	
1972				
15 May	Amber		.01	
28 May	Amber		.01	
29 May	Red			.05
30 May	Red			.10
31 May	Amber			.10
2 Aug.	Amber		.07	
3 Aug.	Amber		.90	
4 Aug.	Amber		.20	
5 Aug.	Amber		.35	
6 Aug.	Red			.20
7 Aug.	Red			.20
8 Aug.	Red			.30

TABLE VI

ALL FORECASTS ≥ 0.40 AMBER

Forecast for Day + 1

	Amber		Red			Existing
Date	.40-.59	.60-1.00	0-.09	.10-.19	.20-.29	Next Day
1971						
6 April			.05			Green
20 April			.10			Green
12 May	.50					Green
13 May	.40					Amber
14 May					.20	Green
16 May			.10			Green
17 May	.40					Green
01 Sept.	.50					Amber
1972						
15 May			.05			Green
28 May			.05			Red
29 May				.10		Red
30 May				.10		Amber
31 May	.50					Green
2 Aug.		.90				Amber
5 Aug.					.20	Red
6 Aug.					.20	Red
7 Aug.					.20	Red
8 Aug.					.30	Green
1973						
29 April			.10			Green

ESTIMATES OF SST DOSE RATES BASED ON SATELLITE PARTICLE DATA

By utilizing dose transport relations derived by Flamm and Lingenfelter (1964) as tabulated by Haurwitz (private communication), satellite data can be used to estimate SST dose rates. The computer dose relies on total event size well as an energy spectral parameter that is assumed to be exponential in rigidity. The NASA National Space Science Data Center (King, 1972) has tabulated the > 30 MeV and > 60 MeV proton fluxes, as measured by the satellites IMP -- 4 and IMP -- 5 and encompassing the time period May 1967 through August 1972. These energy thresholds are considerably lower than those of particles that contribute to SST doses, so the rigidity spectral parameter must be assumed to be constant from 30 MeV up to several hundred MeV. The results of such a computation are shown in Table VII, which contains extrapolated peak dose rates for all events for which the extrapolated dose rate exceeded one millirem/hour in the 1967 to 1972 interval. Some experimentally measured dose rates from the HARES instrumentation (Philbrick, 1971) have been included for comparison.

For the period of this evaluation -- March 1971 to May 1973 -- there is only one interval, early August 1972, when there was either amber or red conditions. In that interval, the dose rate exceeded 100 millirems per hour for 11 hours on August 4 and amber levels another ten hours on August 4 and 5. Of the five days adjudged red in Part 2, none appears from this data to have been red, while two days adjudged amber should have been red. The series of days in early August illustrates the importance of having a reliable system for estimating the current dose rate and for verifying the forecasts. At the SESC, the primary source of satellite proton data proved to be counting low by almost two orders of magnitude during the early, intense period of the August event. The problem was further compounded when the primary source of ground-level real-time proton data, the polar cap riometer at Thule, apparently saturated so that its peak absorption was only about one-fourth to one-half what it should have been based on prior calibrations and reasonably accurate event satellite data that became available

TABLE VII

SST PEAK DOSE RATES EXTRAPOLATED FROM IMP SATELLITE DATA

Date	Extrapolated SST Peak Dose Rate (millirems/hr.)	HARES Measurements (millirems/hr.)
18-21 Nov. 68	6.0	
25 Feb. 69	3.0	
30 Mar. 69	2.8	1.8 (30/14GMT)
12-17 Apr. 69	2.1	
2-6 Nov. 69	11.5	
25-29 Jan. 71	6.0	2.1 (25/02GMT)
1-5 Sept. 71	4.0	
4 Aug. 72	351.3	
7 Aug. 72	5.7	

(Contains all events from May 1967 through August 1972 with an extrapolated dose rate greater than one millirem/hour) sometime after the event. Since the absorption varies as the square root of the proton flux, the estimated flux was commensurately in error. As a result of these problems, the SESC was unaware of the true size of the August proton event while it was occurring, and in fact, believed it to be about two orders of magnitude smaller than it was. The "amber" existing conditions for 02-06 August reflect the same erroneous information. The need for a reliable real-time proton flux sensor seems to be obvious in cases such as this.

SOME OTHER SESC RADIATION FORECAST EFFORTS

For the last few missions of the Apollo series, SESC was a prime contractor to provide radiation support for the manned mission periods. The general mode of operation was on a short-term basis. Were a major solar flare to occur, the available real-time parameters measured by ground-based sensors and supplemented by some satellite data, would be used to predict the time profile of any resulting radiation dangers. The time period immediately following the flare (1-3 hours) could be used to prepare alternate flight plans that would minimize crew exposures. Implementation of these alternate flight plans were to be delayed until spacecraft sensors confirmed the existence of a proton event. Essentially, the technique consisted of predicting a time varying profile and an event spectral parameter and using these along with dose transport calculations to compute a temporal dose profile. An example of such a profile is shown in figure 20. The predicted curve includes optical and radio data for flares on 02, 04, 07 August 1972. A new prediction was made as each new flare occurred. Though satellite measurements of particle fluxes subsequent to each flare can be used to improve the projected dose rate curve, no such modification is included in figure 20.

By using the same assumptions and computations made in Part 4. the routines used in the Apollo effort could be used to make similar short term SST dose predictions. An important aspect of these routines

SPACE SUIT SKIN DOSE RATE

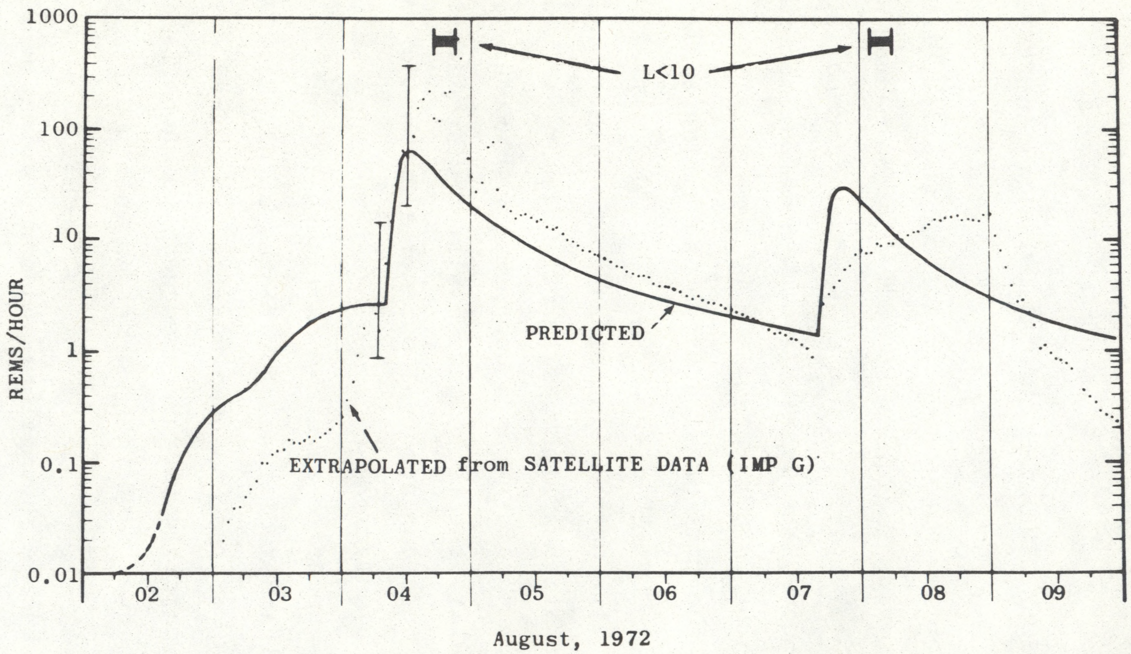

Figure 20

is the use of simple diffusion models to reduce the false alarm rate. Such models, when combined with improved flare forecasts, could be used for longer term predictions. The current development of solar flare models that give quantitative estimates of the energy stored in any active region configuration suggests that such models may become useful forecast tools in the next 2-3 years.

ACKNOWLEDGMENTS

The authors are pleased to acknowledge the substantial contribution of G. Heckman and T. B. Gray to this section, and to R. Doeker for helping to define the data sources of the Space Environment Services Center. Our thanks also to M. Wiarda for assistance in assembling this report.

REFERENCES

Brier, G. W., Verification of forecasts expressed in terms of probability, Monthly Weather Rev., 78, 1, 1950.

Clay, J., Proc. Acad. Sci., Amsterdam, 30, 1115, 1927.

Flamm, E. J., and R. E. Lingenfelter, Neutron and proton dosages in the upper atmosphere from solar flare radiation, Science, 144, 1566, 1964.

Juday, R. D. and G. W. Adams, Planet. Sp. Sci., 17, 1313, 1969.

Kane, S. R. and A. J. Masley, The relationship between polar riometer and space measurements during solar cosmic ray events, McDonnell Douglas Astronautics Co. Paper, WD-1030, 1972.

King, J. H., Study of mutual consistency of IMP-4 solar proton data, National Space Science Data Center, NSSDC 72-14, 1972.

McDonald, F. B., Solar proton manual, NASA-TR-R-169, 1963.

Philbrick, R. B., Natural radiation hazards at high altitude, Air Force Weapons Lab., Tech. Rept., AFWL-YR-72-74, 1972.

Sanders, F., On subjective probability forecasting, J. Appl. Meteorol., 2, 191, 1963.

SESC (Space Environment Services Center), Informal data archives.

Svetska, F., Solar flares, D. Reidel, Holland, 1976.

Webber, W. R., A review of solar cosmic ray events, NASA SP50, 215, 1964.

Williams, D. J., Physics of solar planetary environments, Proc. Int. Symp. Solar-Terr. Phys., AGU, 1976.

Part II

AN FAA POLAR FLIGHT SOLAR COSMIC RADIATION FORECAST/WARNING COMMUNICATION SYSTEM STUDY

AN FAA POLAR FLIGHT SOLAR COSMIC RADIATION FORECAST/WARNING COMMUNICATION SYSTEM STUDY

This paper reports on a forecast message distribution system developed in conjunction with solar cosmic radiation forecasts and warnings of the Space Environment Laboratory of the National Oceanic and Atmospheric Administration for the Federal Aviation Administration's (FAA) Office of Aviation Medicine. The study analyzes the currently available and future aeronautical telecommunication system facilities to determine an optimum system to distribute forecasts to the preflight planning centers in the international flight service stations for polar-flying subsonic and supersonic transport (SST) type aircraft. Also recommended for the system are timely and reliable distribution of warnings to individual in-flight aircraft in polar areas by the responsible air traffic control authority. Multiple transmission of the warning by broadcasts through the FAA, Aeronautical Radio, Inc., and the U.S. Coast Guard Loran-C communication facilities would increase the reliability of warning delivery. The study and recommendations include a future system, aeronautical satellite (AEROSAT), which would give warning message delivery to aircraft with excellent reliability.

Key words: Radiation forecast dissemination; radiation hazard warning; telecommunications system study.

1. INTRODUCTION

During the U.S. space program, the protection of space flight crews from harmful solar radiation of high energy particles became important. Similarly, with the advent of programs for the development of supersonic aircraft to operate at high altitudes for civilian air transportation, it was recognized that exposure of aircraft occupants to galactic and solar cosmic radiation needed investigation. Among other national and international organizations studying the problem, the Office of Supersonic Transportation and the Office of Aviation Medicine of the Federal Aviation Administration (FAA) attempted to analyze available information on cosmic radiation and instituted a program of radiation measurement. In 1967 the Advisory Committee on Biology Aspects of the Supersonic Transport (SST) was appointed. The committee was to monitor and coordinate the High Altitude Radiation Environment Study (HARES) being conducted by the FAA, promote a number of research studies, obtain the best information available on cosmic radiation, and advise the FAA on operational and regulatory measures that would be required to deal with SST radiation problems. Although the U.S. SST program was discontinued in 1971, the FAA maintained the committee until 1974 to complete the tasks for which it had been appointed. The most important reasons for continuing the committee were to prevent the loss of unique and valuable scientific data that were being collected, to protect U.S. citizens who would be flying on supersonic aircraft developed by other nations, and to prepare for the possibility that the United States might sometime acquire supersonic aircraft which would operate under the jurisdiction of the FAA. It also had become evident that radiation exposures in subsonic jets could subject a much larger population to radiation doses equal to or greater than those in the SST's for the same distance traveled.

The FAA has asked the Space Environment Laboratory (SEL) of the National Oceanic and Atmospheric Administration (NOAA) to study and devise a radiation forecast and warning system. As a part of this effort, the Institute for Telecommunication Sciences (ITS) has studied present and future methods of disseminating the forecasts and warnings. The findings are reported here.

1.1 Polar Flight Radiation Hazards

The high energy particles which are responsible for the problem come from the steady (slowly varying) galactic radiation and from solar cosmic radiation during the eruption of solar flares. The magnetosphere surrounding the earth protects the near surface of the earth from the energetic particles except at the polar regions (latitudes greater than about 50°). Near the poles, the particles are able to travel down vertical magnetic field lines to jet flight altitudes before their energy is dissipated by the air. Radiation levels in the polar regions can reach hazardous levels during periods of intense solar cosmic activity. These events occur as the solar activity increases or decreases rapidly near maximum activity. Periods of events with hazardous levels occur on the average of once or twice per year during this part of the solar cycle (11 years), or a total of 5-10 times during each solar cycle.

The final report of the Advisory Committee on "Biology Aspects of the SST," by Rossi et al. (1975), issued in conjunction with the National Council on Radiation Protection and Measurements and the International Commission on Radiological Protection, recommended that the dose limit be a maximum dose equivalent index not to exceed 500 mrem (milli rem) in any one-way flight. It also recommended that SST aircraft carry radiation detection devices on board to show the accumulated dosage during each flight. In-flight warnings of potential high radiation, in conjunction with the measurement devices, would make it possible for the pilots to determine when it would be necessary to decrease altitude to keep exposures within the designated limits.

1.2 Present Forecasts for SST Flights

The National Oceanic and Atmospheric Administration's Space Environment Laboratory (SEL) has devised a system of solar cosmic radiation forecasts and warnings, made by extrapolating from current conditions. It is assumed that these conditions will continue until some forecast input indicates a change. Actual current conditions are monitored from solar optical observations of flares around the world and particle counts from satellites. These are incorporated into the forecasts.

The Space Environment Laboratory has been making daily radiation forecasts for the Royal Aircraft Establishment's Concorde program since 1969. These SOLTERWARN forecasts are issued at 2200-2300 UT. The message consists of one color word followed by a decimal point and two digits for each of the three days; e.g., amber .10.10.10. The current value of the radiation dose rate equivalent at 50,000 to 60,000 ft (15,000 to 18,000 m) altitude at 50° N. geomagnetic latitude is given in terms of a color-code range:

Green = < 10 mrem/hr,

Amber = 10 to 100 mrem/hr, and

Red = > 100 mrem/hr.

The second part of the forecast is the confidence factor that amber or red conditions will exist on the next and following two days. The red condition is presently considered to be the action level.

It is planned that the new SOLTERWARN forecasts for the FAA will be updated when warranted rather than issued once a day. A warning is to be given when a change in the forecast is such that immediate action is required. Since a warning does require timely action, the system used for disseminating forecasts and warnings must give a high priority to warnings.

1.3 Present Communications for SST Flights

The SOLTERWARN forecast message for the Concorde is telephoned daily to the FAA's Denver Flight Service Station (FSS). The Denver FSS is the local input point to the Weather Message Switching Center (WMSC) in Kansas City, Kansas. The WMSC is the central switching point for the FAA's teletype message network. This network, described in Appendix A, also includes access to international air traffic control communications networks (IATCS). The present forecasts are routed from Kansas City to London, England, for use in Concorde Flight planning.

2. REQUIREMENTS

Requirements exist to transmit forecasts and warnings from the Space Environment Laboratory, Boulder, Colorado, to various locations in the U.S. and abroad, and to aircraft in flight on transpolar routes (fig. 21). Warnings must be prepared and disseminated in time to allow flight operations to be altered to avoid exposure of passengers and crew to excessive radiation.

Solar activity causing increases in high latitude cosmic radiation levels of sufficient magnitude to constitute a hazard to personnel in commercial aircraft is infrequent (Part I, table VIII), averaging several events per year, although events are by no means uniformly spaced in time.

Operations in the transpolar regions include aircarrier, general aviation, and military aircraft. However, for practical purposes, distinctions between these classes are not substantial since all are expected to be operating under instrument flight rules (IFR) where control is exercised by the various Air Traffic Control agencies. All will have the minimum complement of avionics equipment required under IFR procedures.

Both forecast and warning messages are very short. The forecast is a five-word plus address message described in table VIII. The warning requires only one word plus address.

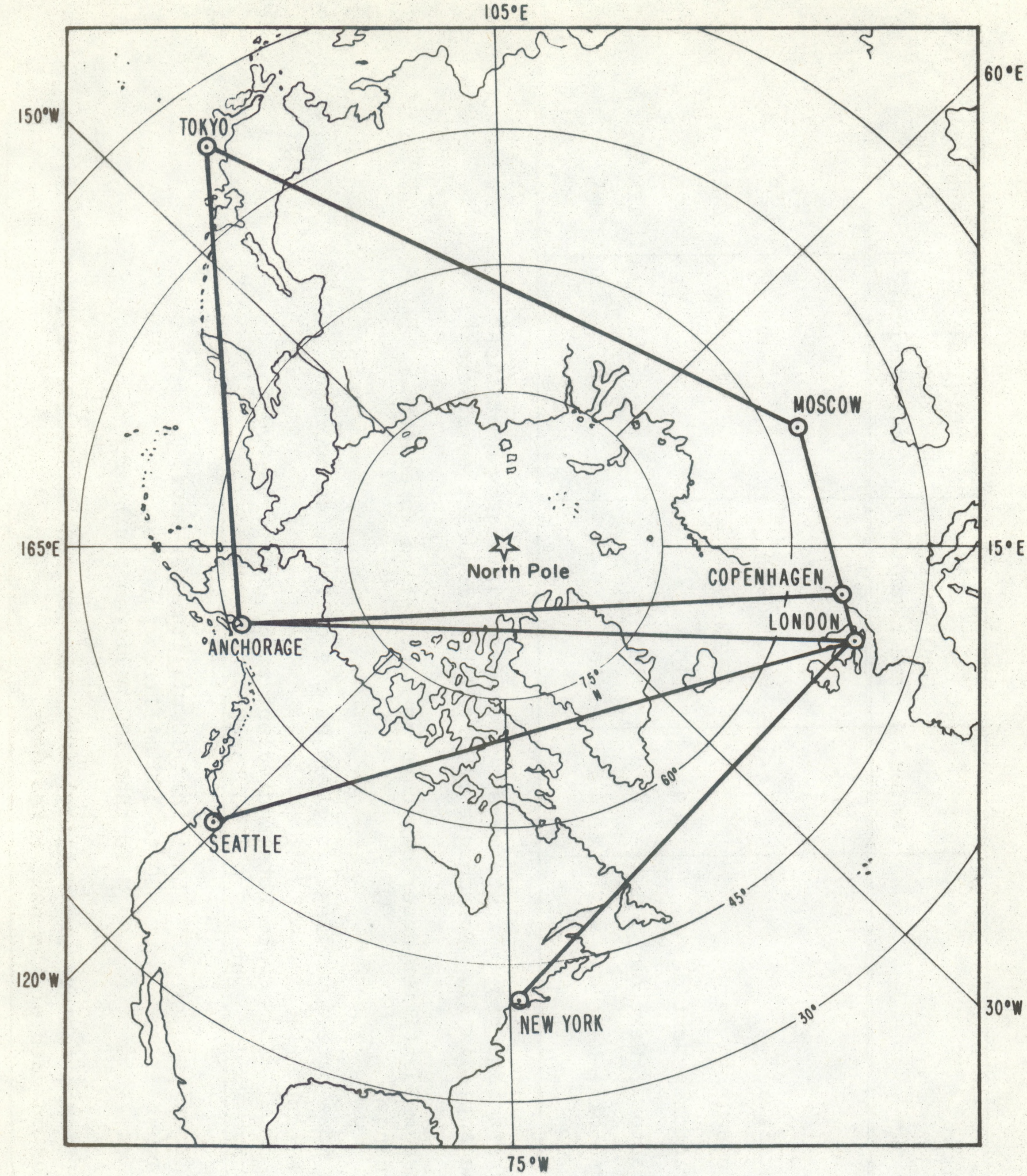

Figure 21. Representative polar region air routes.

Table VIII. Forecast Message Structure

	Notes	Oral Text, and Example	Digital Form (No. of Bits)	Analog Form
Address	1			
Message Identifier	2	SOLTERWARN		
Dose Rate Equivalent	3	GREEN	2	GREEN
Confidence Factor - Next day	4	.10	4	TEN
Confidence Factor - Next day + 1	4	.10	4	TEN
Confidence Factor - Next day + 2	4	.10	4	TEN

Note 1. Address required to route message to appropriate ground station (see Appendix A). No address required for broadcast to aircraft.

Note 2. Message Identifier describes this as a radiation forecast or warning.

Note 3. The dose rate equivalent is given as one of three categories:

Message Word	Dose Rate Equivalent at 50,000 to 60,000 ft, at 50° N. Geomagnetic Latitude
Green	Less than 10 millirem per hour.
Amber	10 to 100 millirem per hour.
Red	More than 100 millirem per hour.

Note 4. Confidence factor (probability) that amber or red conditions will exist on each of the next three days.

Delivery time is here defined as the time lapse between the preparation of a forecast or warning and its reliable receipt by intended addressees. Delivery time for forecasts is not critical, but as much advance notice as is feasible is desirable. For planning purposes, a delivery time of not more than 30 min is suggested. This provides for delivery of the updated forecast prior to the start of the first day for which the forecast is valid. Delivery time for warnings is critical and must be as short as possible.

Total flight duration for air carrier operations through the polar regions are less than 4 hours for SST aircraft and up to 8-10 hours for subsonic-turbojet aircraft. These times are for the total flight, a fraction occurring in polar regions.

The period in which delivery of forecasts and warnings is most important extends from the time when the forecast is issued until the onset of high radiation levels, at which time instruments in the aircraft will provide the warning. After the flare starts, only minutes are available before radiation arrives at the earth. The minimum time for solar cosmic radiation is usually a half hour to an hour as reported by Hakura and Goh (1959), Bailey (1964), and Pope and Grubb (1972).

Descent to lower altitudes, alternate routing, or flight cancellation to avoid predicted hazards all impose operational and economic penalties that are to be avoided whenever possible. Thus, false alarms are to be minimized. Consideration of false alarms in the basic warning process is beyond the scope of this report. However, the communications system must avoid the distortion of radio messages that might be interpreted falsely on receipt.

3. EXISTING COMMUNICATIONS

The communications system is most conveniently considered in two segments. The first provides for distribution of forecasts and warnings from their point of origin to various ground stations. The second segment transmits information from the ground stations to aircraft in flight. The requirements for each segment are substantially different as are the facilities with which to meet them.

3.1 Distribution to Ground Stations

An extensive communications network already exists for both national and international distribution as described by Hanson et al. (1973). The Aeronautical Fixed Telecommunication Network (AFTN), summarized in Appendix A, provides teletype message delivery between the Denver Flight Service Station (FSS) and aviation ground stations in the United States and Alaska within 30 seconds of receipt. Warnings are presently telephoned from the Space Environment Laboratory, Boulder, Colorado, to the Denver FSS. This total process presently requires from 2 to 20 minutes, depending on the workload at the Denver FSS.

The ground stations of future interest are at the Aeronautical Control Centers (ACC's) and Flight Information Centers (FIC's) with responsibilities for polar flights. These are located at New York; Oakland, California; and Anchorage, Alaska. In addition, forecasts will be needed at all airports from which transpolar flights depart and at the airline operating companies or agencies.

Message delivery to U.S. and International Air Traffic Control facilities is easily accomplished through the AFTN discussed above. Distribution of messages to additional facilities as transpolar flights originate at additional airports is also easily accomplished via this network at no increase in delivery time. For flight operations out of the U.S., Aeronautical Radio Incorporated (ARINC) provides a single, centralized point for distribution of company communications, both to ground points (airports) and to aircraft in flight.

3.2 Communications to Aircraft in Flight

The U.S. and other countries operate a wide range of communications, navigation, and surveillance systems which are potentially capable of carrying warning messages to aircraft in flight. The two most obvious systems are the high frequency (HF) and very high frequency (VHF) voice communication systems. These two are discussed here and in the appendices with others. Other systems which offer equal or lesser potential are not considered, although some might offer operational advantages as alternatives to the two main systems. Very high frequency omni-ranges (VOR's), for example, may be used to broadcast warnings in conjunction with the transcribed weather briefings (TWEB's) already broadcast. These facilities offer no greater (and sometimes less) capability to communicate than the VHF voice system, but could be included in the proposed system for redundancy.

Existing VHF voice communications systems provide the necessary reliability and speed of delivery, but only in areas within 250 to 400 nmi (463 to 741 km) of the gateway cities. At longer ranges, HF radio provides the basic communications to aircraft in flight, but with substantially reduced reliability during periods of ionospheric disturbance--particularly in polar regions. Thus, HF radio is likely to offer less service during the periods when it is most needed for distribution of warnings. On transoceanic flights in the North Atlantic, for example, International Civil Aviation Organization (ICAO) figures show that as many as half of aircraft position reports are missed when propagation conditions are poor. Three quarters of the remainder were as much as six minutes late. At high latitudes, HF radio is even less reliable, but it is still the only service presently available.

One possibility exists to improve the performance of the HF radio system for warning distribution without major changes in ground equipment or avionics. Signaling tones may be used to transmit a digital message, perhaps by employing the presently used SELCAL system (see Appendix B). In both cases, improvements depend on the simplicity of the warning message--essentially a one-word or one-bit message. If the message is coded and transmitted as an audio tone, then a 10 dB improvement in detectability can be achieved. This improvement is not sufficient to maintain communications at all times, but will improve reliability.

4. FUTURE COMMUNICATIONS

The ground system presently available will continue to serve in the future and, for warning dissemination, should prove adequate. Improved access and distribution time is possible by establishing direct teletype input facilities with appropriate priority at SEL, Boulder if that becomes necessary.

The major goal for future communication systems is the improvement of coverage and reliability of the air-ground service. This is a continuing concern for air traffic officials, and a major development program (AEROSAT) is underway to provide equatorial and mid-latitude coverage via satellite.

The Aerosat system (OSEM, 1974) will consist initially of a single synchronous satellite to be deployed at the equator after about 1978 for experimentation and evaluation. The system includes an aeronautical services earth terminal (ASET) for North America, provided by Canada and the U.S. at the FAA's National Aviation Facilities Experimental Center in New Jersey, and another ASET in Europe. About a year later a second satellite will be positioned that will provide the capability for two lines of position for the ranging portion of the surveillance program. The aircraft altitude telemetered by the data link and the intersection of the lines of position define a unique position in the northern or southern hemisphere. The AEROSAT system will begin testing with dedicated aircraft a few months after satellite launch, then expand initially to 20 commercial aircraft for the first few years of operational experimentation and evaluation. The system will provide voice quality comparable to the existing VHF communication system and provide data transmission at 1200 and 2400 bits per second with an error rate of about 10^{-5}.

The plan and memorandum of understanding specify two satellites at 15° and 40° W. longitude with VHF (125.425-125.975 MHz) and L band (1543.5-1558.5 MHz) voice and data transmission down to the aircraft. The return transmission to the satellite is on 131.425-131.975 MHz and 1645-1660 MHz. Then the satellite relays the voice and data to the ground ASET on 5125-5250 MHz, with the uplink from the ASET on 5000-5125 MHz. At an elevation angle of 10° to the satellite, the coverage in the polar region will be to 70° N. latitude for L band and to about 82° for VHF. The U.S. will provide an aeronautical satellite communication center for satellite control and to feed information to an oceanic control center (OCC). SELCAL capability will be provided within the system.

Direct ATC voice communication by the satellite can be maintained with the air crew in flight, eliminating the communicator go-between of the existing HF communication system. Some warning distribution limitation can be foreseen even with the AEROSAT system. Initially it is to be provided only for the North Atlantic air routes, with possible expansion with other satellites for North Pacific air routes. Another limitation is the lack of complete coverage of the polar area. At present the L band frequency part of AEROSAT appears to be receiving the greatest development and yet has more limited polar coverage.

However, notice in figure 21 that no known air route now traverses the region above about 85°. Signal propagation to and from satellites is affected by the variabilities of the ionosphere, particularly at VHF. Propagation also is affected by the synchronous orbit problem of the direction of propagation coinciding with the sun (looking into the sun), which increases the noise level for a few hours daily near equinox seasons of each year. Solar radio noise outburst also affect the noise level in a way similar to the VHF case discussed in Appendix B. An additional signal margin allowance (at least 10 dB) for these three effects must be made in the AEROSAT system design (OSEM, 1974), to retain the 10^{-5} error rate specified. However, for polar routes, AEROSAT will be operating near the design limits of area coverage with good signals even when the additional allowance is included.

Domestic and military satellites are becoming available that could conceivably provide service to the polar regions. The use of these satellites to provide forecast and warning dissemination would involve much technical, economic and production planning. For example, some problems are groundbased and airborne equipment for the service would be costly additions to COMSAT equipment and the satellites are usually dedicated to specific commercial and military services.

Other navigation and surveillance systems capable of communicating warnings are under development, but these systems will not serve polar regions. Alternatives of potential value are the long range navigation systems. The Omega and VLF navigation systems were considered. Omega by international agreement cannot be used for communications. VLF is a classified military tactical system which cannot be utilized for this purpose.

5. THE RECOMMENDED SYSTEM

The recommended procedure and telecommunications vehicle for the distribution of the forecasts and warnings of solar cosmic radiation issued by the NOAA/SEL Forecast Center are summarized in the following. A differentiation is made between forecasts and warnings at the time the forecast hazard level becomes red. The red level is the ACTION level since a radiation-producing flare and radiation levels greater than 100 mrem/hr are imminent. At this time a warning is issued by SEL. Forecasts are issued daily and are updated at any time that the hazard level changes.

The forecast/warning is telephoned by the SEL forecaster to the Denver FSS. The FSS routes the forecast/warning message via the 100 WPM teletype Service B to the WMSC/IATSC in Kansas City, where it is automatically switched to the high speed AFTN circuits utilizing telpak circuits to New York, channel 086 and 089 to San Francisco, and from there cable 8060 to Anchorage (fig.22. Computer automatic switching is provided at San Francisco and Anchorage by including AFTN routing indicators for the IFSS destinations at San Francisco, Anchorage, and New York. The message transmission time to the IFSS's receipt is about 0.5 s. The IFSS's are responsible for updating the briefing information and the transcribed broadcast tapes for TWEB on VOR's and NDB's.

When a forecast is red and a warning issued, the same procedure is used as for a forecast plus adding ACC routing indicators and the higher priority, SS, for message delivery to Oakland, Anchorage, and New York. When a warning is received at the ACC, the three ACC's, using SELCAL, immediately contact the aircraft under their control with the change in hazard level and remain in standby communications until the GO or CLEAR is received from SEL. Both of the VHF and HF communication systems are utilized for contact depending upon the aircraft range, channel availability, and radio propagation conditions.

The warning also should be broadcast to all aircraft utilizing the TWEB broadcast systems available to the IFSS. Another warning message broadcast channel is the Loran-C communication system. The U.S. Coast Guard Headquarters Operation Office needs to be telephoned by the SEL forecaster at the same time as the Denver FSS. Aircrews could then receive the warning status on the Loran-C solar cosmic radiation monitor indicator during a red forecast. Thus, by using all systems available, redundancy is utilized to increase the reliability of warning delivery to the inflight aircraft.

The forecast/warning message should consist of all English words written out and repeated to increase redundancy. Then, even though a few letters could be in error, the meaning of the message will be retained. High frequency radio systems and the lack of error control on AFTN require this message form for best reliability.

For the future, the same type of forecast/warning message could be routed through AFTN to the OCC and the satellite radio channel utilized to warn and control the aircraft. The forecast/warning message format needs only

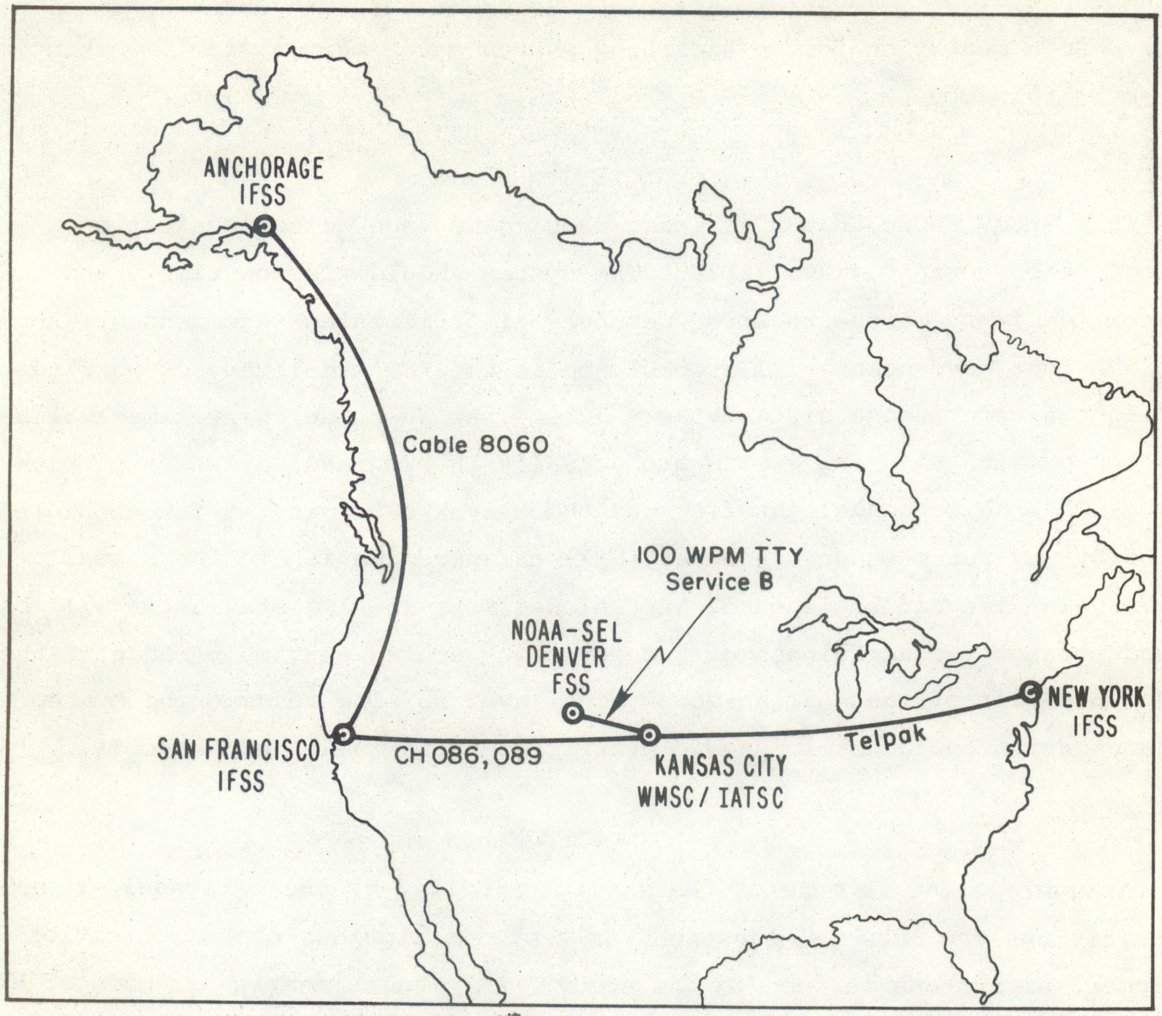

Figure 22. FAA telecommunications for forecast distribution to IFSS.

to be changed by software program changes in most newly proposed telecommunication systems to obtain new routing or handle new message types. The solar cosmic radiation forecast/warning system can remain a viable working system in this way.

6. CONCLUSIONS

This study shows that a forecast/warning message telecommunication system can be currently available. The system should provide timely and reliable delivery of the required messages if utilized as recommended. Any problems that may appear will probably be in the ACC's delivery of warnings to in-flight aircraft some distance away during the short delivery time available (see Appendix B) when the events are actually in progress; a lesser problem is the NOAA/FAA personnel interface at the Denver FSS. The system should be tested by dry-run messages; however, only an approximation to the actual delivery-in-time can be learned. Actual delivery-in-time statistics will be needed to show the usefulness of the forecast/warning service because of the random behavior of these solar-geophysical events. The recommended system implementation could develop these statistics in the next few years.

7. ACKNOWLEDGMENTS

Acknowledgment is made of the service provided by the personnel of several organizations who answered questions or sent descriptions of communication equipment or systems for use in the study. Particular mention is made of Mr. Climy and Mr. Dick Correll of ARINC, Inc.; of FAA's Mr. Dave Gray, Chief of the Anchorage IFSS, and Mr. Wayne Brimner, Chief of the Denver FSS; of Lt. Commander Bill Schorr of the U.S. Coast Guard Loran Operations Office; and of Mr. Walter Dean of Magnavox Corporation for information on the Loran-C communication channel. Appreciation is given to Ms. Jane L. Russell and Ms. Renee Horowitz of ITS for assistance in preparation of the report.

8. REFERENCES

Bailey, D. K. (1964), Polar-cap absorption, Planetary Space Science 12, 509.

Hakura, Y., and T. Goh (1959), Pre-SC polar cap ionospheric blackout and type IV solar radio outburst, J. Radio Res. Lab. 6, No. 28, 639-641.

Hanson, J. C., E. M. Boseck, R. Weber, and R. Laxence (1973), FAA communications system description, Final Report FAA-RD-73-36, DOT/FAA Systems Research and Development Service, Washington, D.C. 20591.

OSEM--Office of Systems Engineering Management (1974), Engineering and development program plan - Aeronautical satellites (AEROSAT), Report No. FAA-ED-17-2, DOT/FAA Systems Research and Development Service, Washington, DC 20590.

Pope, J. H., and R. N. Grubb, Editors (1972), Effects of solar disturbances on radio communications with aircraft, NOAA Tech. Rept. ERL 233-SEL 22.

Rossi, H. H. (1975), Cosmic radiation exposure in supersonic and subsonic flight, Advisory Committee for Radiation Biology Aspects of the SST, Final Report, Aviat. Space Environ. Med. 49, No. 9, 1170-1185.

APPENDIX A. A SUMMARY DESCRIPTION OF THE AERONAUTICAL FIXED TELECOMMUNICATION NETWORK

The Aeronautical Fixed Telecommunication Network (AFTN) is an integrated world-wide teletypewriter system of aeronautical fixed circuits. The purpose of AFTN is to provide communication service for international aircraft movements (i.e., administrative messages and meteorological data concerned with the safety of air navigation) and promote the regular, efficient, and economical operation of air services.

Specific features of interest for warning distribution include:

1) Maximum size of messages--text limited to 200 groups (words).

2) Format restrictions (five divisions: heading, address, origin, text, and ending (and shortened address may be included)).

3) Speed of delivery (maximum delivery time, not greater than 5-10 minutes).

4) Priorities:

   SS, Emergency-affecting safety of life and property.

   DD, Special priority handling.

   FF, Concerning control and movement of aircraft, flight safety.

   GG, Flight regularity messages and meteorological forecasts.

   JJ, Administrative--meteorological observations.

   KK, Reservation.

   LL, Company and operating agency messages.

5) Routing information (typical):

	IFSS Routing Symbol	ATC Routing	NOTAM Office
Anchorage IFSS	PANCYF	PAZAZQ	PANCYN
New York IFSS	KJFKYF	KJFKY-	KJFKJN
San Francisco IFSS	KSFOYF	KSFOY-	KJFKJN

APPENDIX B. SYSTEMS FOR COMMUNICATING WITH AIRCRAFT IN FLIGHT

As mentioned in the main text, a number of telecommunications systems might provide the mechanism for delivery of forecasts and warnings to aircraft in flight. Functional descriptions and pertinent technical characteristics of two are summarized in table B1.

Table B1. Air-Ground Communications Facilities

1. Very High Frequency (VHF) Radio

Frequencies: 108-136 MHz.

Modulation: Double sideband, AM and SELCAL.

Capacity: Voice channel.

Reliability: Good-excellent.

Maximum time required to deliver a priority message to an IFR aircraft: < 1 min.

Range - Radio line of sight (250 nmi (463 km) for an aircraft at 40,000 ft (12,000 m)): Extended range VHF radio provides service at ranges up to 400 nmi (741 km).

Susceptibility to Ionospheric Disturbances: Very low (4 dB loss in signal-to-noise ratio experienced in solar noise storms).

Notes: These facilities are located to provide 100 percent coverage at en-route altitudes in the coterminous United States and most of Western Europe. However, they do not provide adequate coverage for over-water flights or polar regions. Some stations operated by ARINC utilizing high power and high gain antennas have extended this range, but results are still not satisfactory for reliable long-range coverage beyond 400 nmi (741 km).

2. High Frequency (HF) Radio

Frequencies: 3-30 MHz (see fig. B.2).

Modulation: Double and single (upper) sideband, with full and suppressed carrier, AM and SELCAL.

Capacity: Voice channel.

Reliability: Good--poor during some geophysical events.

Maximum time required to deliver a priority message to IFR aircraft: 1 minute to 10 minutes if at all possible.

Range: Over the whole polar air route, but over half the route with the best reliability.

The VHF Voice Service

The VHF voice service may be used to provide warnings to aircraft during their first half hour of flight from departure points or while over those land masses with coverage.

Along air routes within the U.S. and Canada, VHF communication and navigation systems in the aeronautical mobile band from 108-136 MHz are the major systems used. Very high frequency radio is mainly limited to line-of-sight signal propagation. A great number of remote and VOR communication sites are used along a route. High terrain sites, where possible, and the normal flight altitudes make possible up to 150-250 nmi (278-463 km) of line-of-sight ranges. By the use of high gain beam antennas, high power transmitters, and judicious use of mountain-top sites, VHF communication is extended to about 400 nmi (741 km) from land on some ocean routes. Very high frequency communication at greater distances from land is not available, except for an occasional weather-communication ship. Similarly, in the polar regions, VHF communication sites are scarce. Canada, Greenland, and Iceland's VHF communication sites fill in some areas. In other areas HF radio provides the only service.

Double sideband AM voice (6A3) modulation is used in the VHF aeronautical band. Ground station selective calling (SELCAL) to a particular aircraft is also available by an audio tone-coded transmission on the 6A3 or 3A3H modulation mode. The ICAO SELCAL is two consecutive tone pulses (1 ± 0.25 s duration and 0.2 ± 0.1 s interval) with each pulse containing equal amounts of two simultaneous audio tones. The tones are any combination of 12 logarithmically spaced frequencies from 312.6 to 977.2 Hz forming a discrete code. The demodulated tones operate a decoder and indicator in the aircraft to alert the flight crew that they are being paged. The aircraft receiver must be operating on frequency continuously to be ready to receive SELCAL. A voice/data-link system of communication operating on the same frequencies is undergoing testing at this time. The data link operates through minimum-shift-keying modems at 2400 or 4800 bits per second.

The ARINC and FAA both operate VHF communication facilities. The ARINC specializes in air carrier company business within the U.S., extended range VHF from the gateway cities, and along the land portion of the oceanic routes to Alaska and Newfoundland. Most other VHF aeronautical communications that work with polar flights are FAA operated in the U.S. and Alaska.

Very high frequency communication, as it serves only line-of-sight distances, is not greatly disturbed by the solar cosmic ray events of warning concern. However, a type IV solar radio noise emission which arrives in about a minute or so, and lasts for hours to days may increase the noise up to 4 dB. Most VHF communication circuits operate with an signal-to-noise (S/N) ratio which will tolerate this decrease in system margin. However, with the extended range VHF operating for maximum range of communication from land, 4 dB means about a 20 nmi reduction in range. It is hoped that HF will be good enough to fill the longer gap at the time needed.

Areas of air traffic control responsibility are variously referred to as control areas (CTA's) and Flight Information Regions (FIR's). Control agencies in each of these areas (fig. B.1) are also provided with long-range, high-frequency communications facilities. A radio frequency assignment plan has been adopted by the ICAO system to limit interference and allow good frequency usage. Figure B.2 shows the HF assignments to ground stations by areas. Of the U.S. CTA/FIR's, the FAA operates some radio facilities, and Aeronautical Radio (ARINC) operates others. However, both are interconnected within the same WMSC/IATCS communication system. Of the radio facilities usable for polar flights, the FAA operates those in Alaska for the Anchorage oceanic and arctic ATC/FIR. These are in Anchorage and out toward the Aleutian Islands at Cold Bay. The ARINC operates those at San Francisco for the Oakland CTA/FIR, and at New York for its CTA/FIR.

The HF Voice Service

These HF facilities use amplitude modulation in double sideband (6A3) voice and single sideband (upper sideband) voice with full (3A3H) or suppressed carrier (3A3J). The SELCAL (ICAO format coding) is also available along many routes for paging specific aircraft.

The HF radio communication has a problem of reliability because of signal variability. High frequency radio propagation at distances greater than the VHF range of 200-400 nmi (370-741 km) is via the ionosphere. Variations of the ionospheric structure with time cause variations in path distance and attenuation of the radio waves. These variations are seen as variation in signal strength and modulation distortion, commonly known as fading. The polar regions, in particular, are adversely affected by large ionospheric

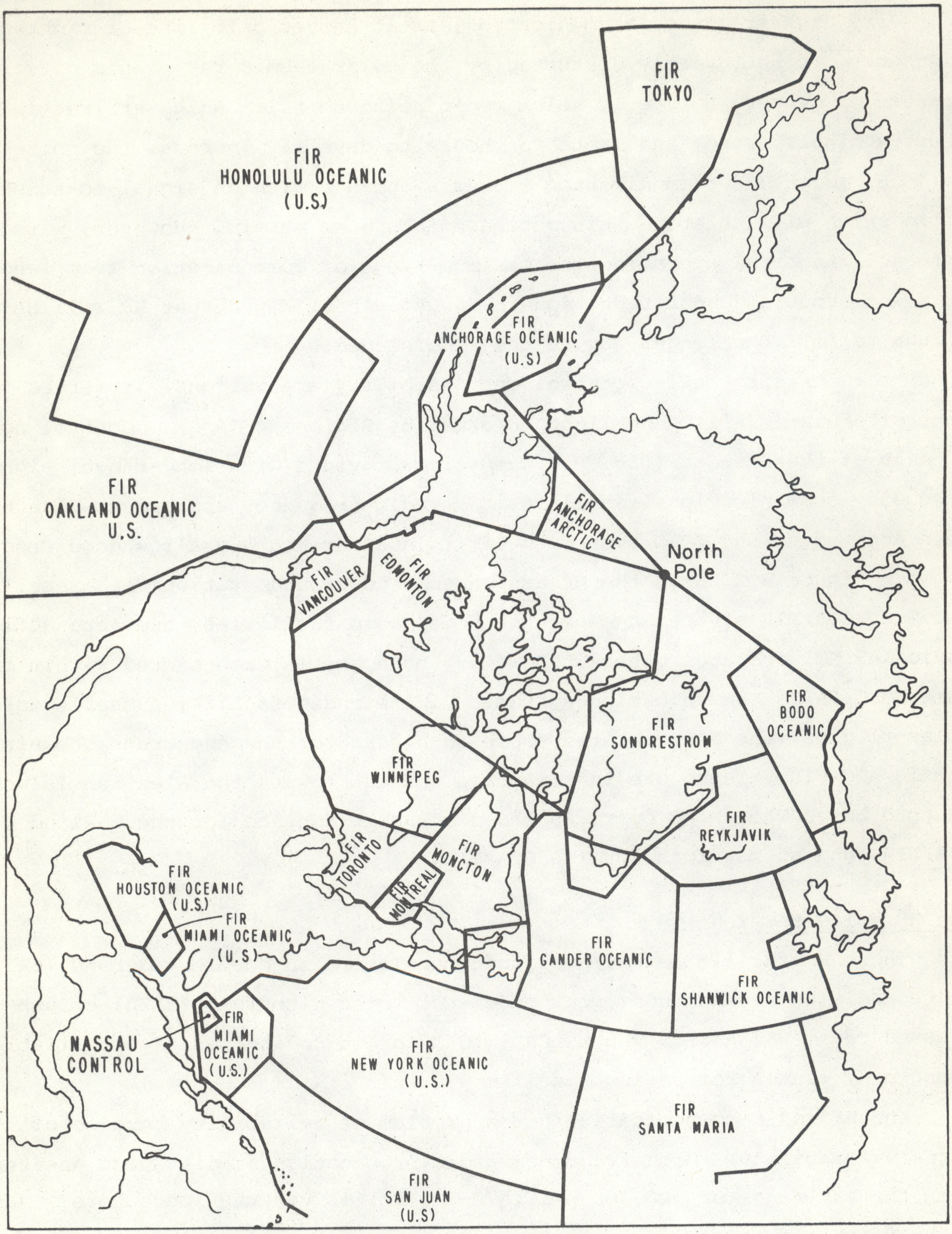

Figure B.1. The oceanic and arctic flight information regions and control areas.

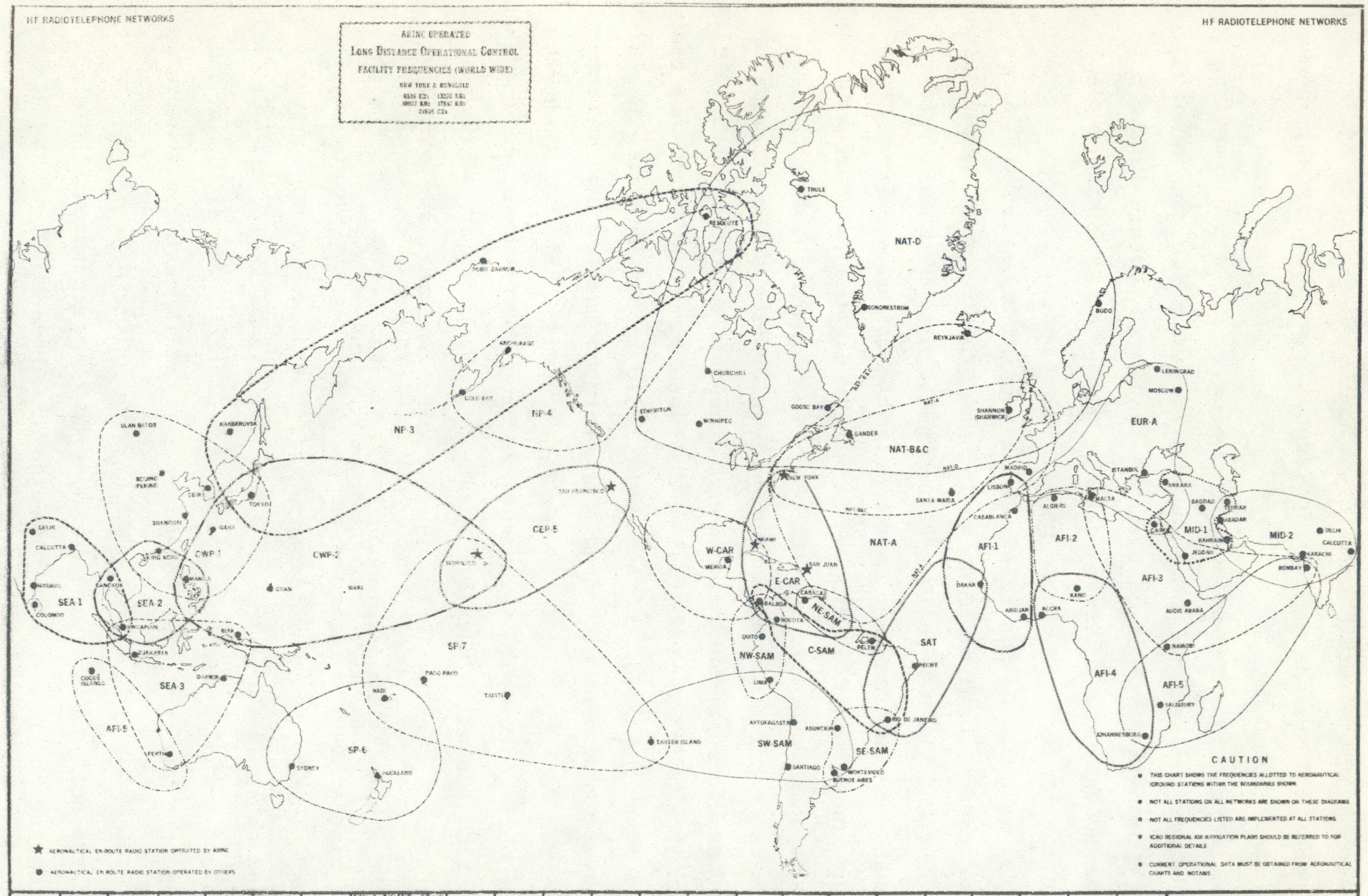

SEA-1	SEA-2	SEA-3	CWP-1&2	NP-3&4	CEP-5	SP-6&7	NW & SW SAM	NE-SE-C SAM	SAT	W-CAR	E-CAR
2987	2868	2987	2896	2910	3001	2945	2889	2910	3432	2966	2952
5673	5624	5673	5505	5589	3467	5638	4696	5582	6610	5568	5484
8882	8840	8868	6631	8938	5554	8847	6666	8847	8882	6561	6540
13288	8868	8854	8854	13264	5603	13304	8826	11327	10049	6568	6568
17965	13312	13288	11303	17909	8875	17909	11343	13320	13344	8840	8959
	17965	17965	13296		8931		17917	17917	17949	10017	11343
			17909		13312					13320	11367
					13336					17925	17925
					17909						

NAT-A	NAT-B	NAT-C	NAT-D	AFI-1	AFI-2&4	AFI-3	AFI-5	EUR-A		MID-1	MID-2
2931	2987	2945	2868	3432	3411	2966	3481	2910		3404	3446
5610	5673	5638	5624	6610	5519	5505	6561	4689		5603	6624
8945	8889	8854	8910	8882	8826	8959	10025	6582		8847	10009
13328	13288	13288	13328	13344	13304	13336	13336	8875		13336	13336
17941	17941	17941	17941	17925	17925	17925	17925	11303			

ALL FREQUENCIES ARE EXPRESSED IN KILOHERTZ

ICAO HIGH FREQUENCY EN-ROUTE RADIOTELEPHONY NETWORKS

SERVING THE MAJOR WORLD AIR ROUTE AREAS

EFFECTIVE 0901Z APRIL 24, 1975

AERONAUTICAL RADIO, INC.

HF-501-1

Figure B.2. HF radio frequency assignment areas.

variations. The HF signal variation during a solar cosmic radiation event, when communication to the aircraft must be available, is a three-part sequence of sudden ionospheric disturbance (SID), polar cap absorption (PCA), and an ionospheric-geomagnetic storm.

The SID begins first as the solar flare emits x-rays which travel in 8 minutes to the lower sunlit ionosphere causing increased ionization with radio wave absorption. A typical curve shape of signal fadeout is shown in figure B.3. The amount of attenuation depends on the sun's zenith angle relationship to the radio great circle path. Polar radio paths would see only about 0.7 or less of the possible sub-solar point attenuation. Atmospheric noise decreases some 5 to 10 dB during the SID tending to maintain the S/N ratio. Even then, the S/N ratio requires that 25 to 35 dB of system margin be available for adequate voice communication. The margin can be maximized during the SID by utilizing a frequency near the maximum usable (MUF) for the distance involved.

The PCA is the polar cap region HF signal absorption/attenuation from the incoming solar cosmic radiation. Signal attenuation starts within a half hour to an hour after the flare beginning, is usually much greater than that of the SID, and often precludes the use of HF radio in the daytime. The HF communication system would have to handle the warning fast enough to reach the aircraft before the PCA; the PCA is caused by the same solar radiation with which the warning is concerned. Forecasts are presently issued 1 hr in advance of the daily period for which they are effective. Warnings are to be issued on the observation of solar activity (flares being imminent, see sec. 1.2, p. 53). Thus, the warning appears about 15-30 minutes in advance of a potential hazard to aircraft. The timing sequence to deliver the warning to the inflight aircraft is of crucial importance. If a typical PCA or solar cosmic radiation influx curve is superimposed upon the curve of the typical SID attenuation (inverse of signal strength) of figure B.3, the critical timing is seen. Figure B.4 shows the two best time periods for HF radio distribution of the warning; the first being preferred if the warning message can be handled with priority. The PCA does subside with darkness to reappear somewhat diminished with daylight during the next two or three days. This aspect of the PCA and the subsequent ionospheric-magnetic storm would affect warning communication

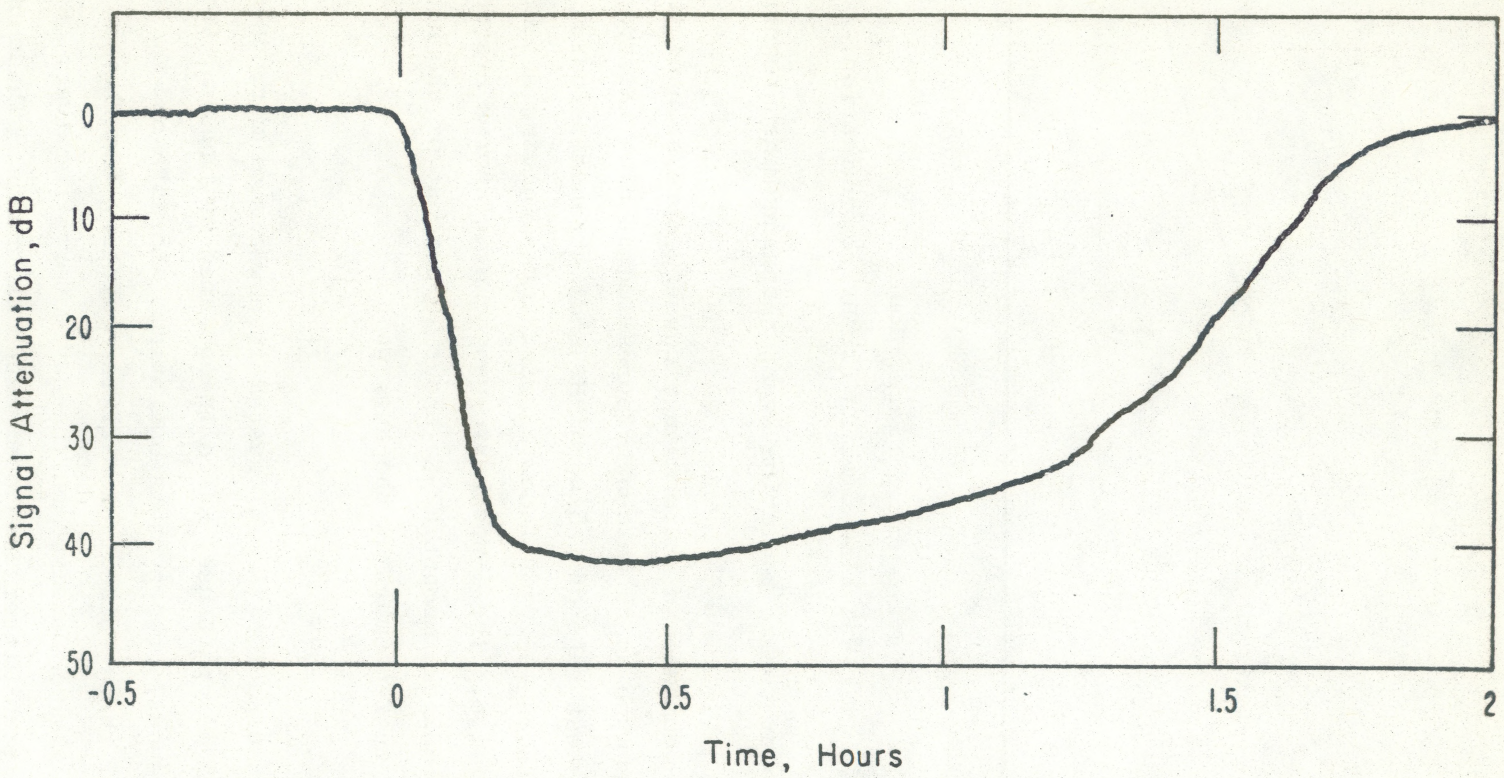

Figure B.3. Typical HF signal fade-out from absorption during a solar flare.

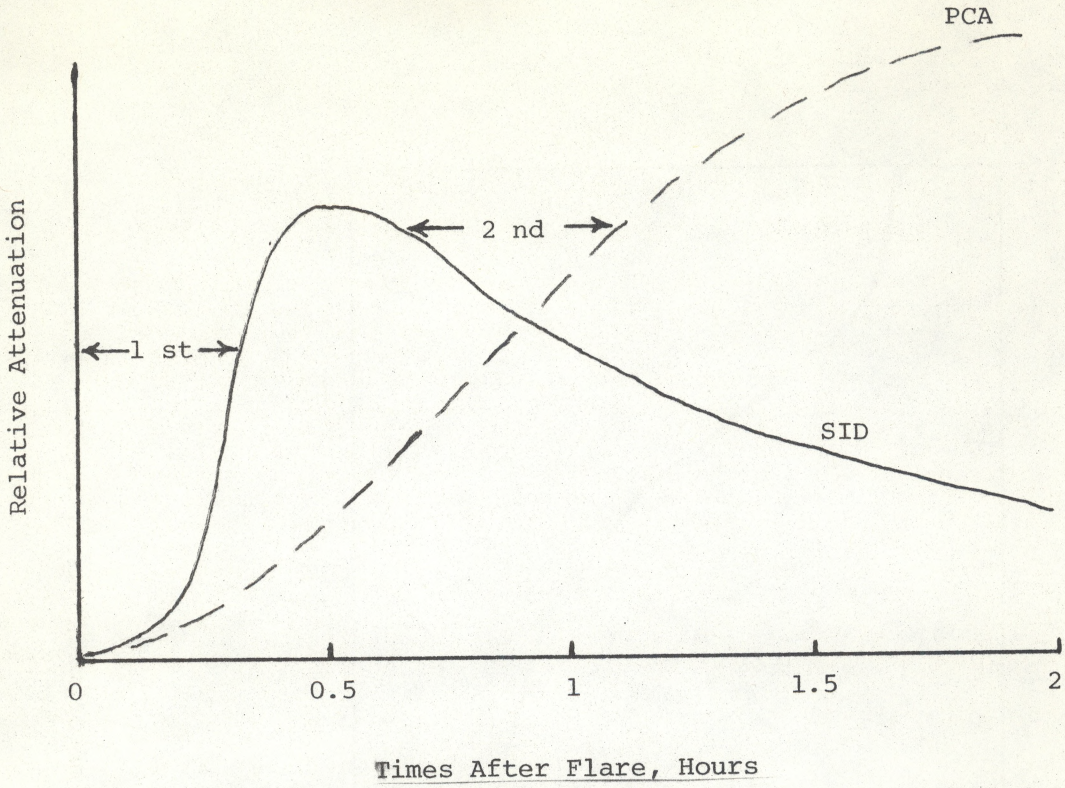

Figure B.4. Critical time periods for HF communication.

only if additional solar cosmic radiation events happened that required successive warnings.

The ionospheric-geomagnetic storm mainly causes depression of the MUF, with the greatest (as much as 30 percent) depression at high latitudes. This storm causes the greatest rate of fading of HF radio transmissions. The signal amplitude averages 10-20 dB fades at fast rates, giving a fluttery sound to voice modulation. The ionospheric-geomagnetic storms are more pronounced near the equinox, amounting to about 10 percent of the hours in March and 20 percent in September on the average.

The Loran Navigation System

The long range navigation (Loran) system is now a medium range navigation system for marine and aircraft use, which is operated by the U.S. Coast Guard. There are presently two systems operating: Loran A and C. A Loran system is composed of three pulse transmitters operating together as a unit to produce a position fix when received on the navigator's receiver. Several pairs or triplets of transmitters are designated as chains. These chains are located along a coast to give coverage of the adjacent ocean and land area.

The three or more transmitters have pulses synchronized as pairs (a master and slave) which give a hyperbolic pulse travel time difference in the vicinity of the two stations. Pulse travel time difference data from the navigator's Loran radio receiver correspond to a line of position for each pair of stations which are shown on charts with hyperbolic grids for each station pair. The navigator's position is at the intersection of the two lines of position.

Loran A operates at about 2 MHz and was built in WW II to cover the coast lines of the Pacific, Atlantic, and Greenland, with a range of up to 900 nmi (1667 km). Loran A is being phased out, starting with the Baffin Bay (West Greenland) chain in the summer of 1975. Each year a chain will be dropped (Alaska and Aleutian Island chains in 1979) until all are gone by 1980. No modification or new work is being considered for Loran A, so it cannot be considered as a candidate.

The air carriers also are considering Loran C as an alternative to an inertial navigation system to provide for redundancy requirements of the FAA. Loran C is a similar system to Loran A, but operates at 100 kHz with greater range (up to 1500 nmi (2778 km)) and better sky-wave propagation characteristics, which allow most of the arctic region to be covered. Loran C has been designated recently as the U.S. national coastal confluence navigation system. Canada is considering a Loran-C system for its arctic region. Of interest to the warning communication problem is a Loran-C communication channel that has been implemented in two forms. A teletype transmission mode, called Clarinet Pilgrim, for Navy operations/information broadcasts to the naval fleet has been implemented on the northwest Pacific chains. The Coast Guard has developed a similar communication and control system for its internal control and monitoring of the chains of transmitters. This system has been installed on the east coast chains and proposed for others. Both systems use pulse position modulation of certain of the eight pulses of a pulse group to form a bit stream for start-stop teletype characters or Morse code CW. A warning message probably can be implemented on this system. However, present aircraft Loran-C receivers may require modification (usually software) to give communication channel output. A fairly simple Loran-C receiver could be developed for the newer aircraft that do not now use Loran C.

Loran-C signal propagation problems are not so well known as those with HF and VHF, but signal amplitude variations do exist. The amount of the variation depends upon the distance to the aircraft, the season, and the time of day. A normal change of up to about 10 dB in amplitude occurs daily at sunrise (to lower signal strength) and sunset (to higher signal strength). In the large SID's, the signal strength first decreases somewhat until recovery begins, then increases greatly. The attenuation effects are not as great as those of HF. As the solar cosmic radiation arrives at earth to produce the PCA, the normal diurnal amplitude change is leveled out by decreasing the night signal amplitude to about the day value. The amount of leveling depends on the size of the PCA. Next the ionospheric-geomagnetic storm affects only the nighttime Loran-C signal by producing rapid-deep fading during the storm recovery phase. Overall, it appears that using the Loran-C system should not present serious difficulty in communicating with the aircraft during the period needed to warn of the imminent solar cosmic radiation event.

Other Communication Possibilities

The other ICAO communication or navigation systems are VOR and Tactical Air Navigation (VORTAC), LF Navigation System (CONSOL), and Non-Directional Beacon (NDB). The VOR portion of VORTAC navigation was included in the discussion of the VHF communication system in this appendix, since the propagation and system operations are largely the same. Some VOR's have the TWEB broadcast, which could be utilized. Areas along polar air routes that should be covered by the solar cosmic radiation forecasts and warnings service do not have VOR service.

CONSOL is a low frequency (about 192-333 kHz) continuous wave system of 10-20° signal lobes or sectors of a circle around each station. A specialized receiver is not required, but the receiver must cover the frequency range and have a beat frequency oscillator. To define the navigator's angle from the station, one counts the number of dots and dashes between equisignals (sector boundaries) as each sector rotates by his position. Most CONSOL stations are located near northwest Europe, the termination of many polar flights. The range is about 1000 nmi (1852 km) over water and propagation problems are similar to those of Loran C. However, there is no communication channel and no development of one is contemplated in the future according to the FAA Internation Navigation Planning Division. Therefore, CONSOL cannot be a candidate.

There are many NDB's at small airstrips in the U.S. (particularly Alaska), Canada, and the northwest European countries. They are the original radio navigation system and are the least costly of the systems. Most aircraft are equipped with automatic radio direction finder receiver systems. However, the accuracy and usefulness is not comparable to the VHF navigation system. A radio transmitter operating in the LF band (200-415 kHz) radiates a nondirectional signal as a radio beacon with a Morse code identification. The aircraft loop antenna, receiver, and indicator are used to show the navigator the direction from the aircraft to the beacon. The range of operation depends on the strength of the radiated signal and is typically 75 nmi (139 km) over land and 350 nmi (648 km) over sea. Propagation problems are essentially those of Loran C.

Many NDB's in the U.S., Alaska, and Canada are used for broadcasting weather forecasts, hourly sequences, etc. continuously and scheduled. The forecasts and warnings should be included.

APPENDIX C. LIST OF ACRONYMS

ACC	Area Control Center
AEROSAT	Aeronautical Satellite
AM	Amplitude Modulation
AFTN	Aeronautical Fixed Telecommunication Network
ARINC	Aeronautical Radio, Inc.
ASET	Aeronautical Satellite Earth Terminal
ATC	Air Traffic Control
CONSOL	LF Navigation System
CTA	Control Area
CW	Continuous Wave OnOff Keying in Morse Code
FAA	Federal Aviation Administration
FIC	Flight Information Center
FIR	Flight Information Region
FSS	Flight Service Station
HARES	High Altitude Radiation Environment Study
HF	High Frequency
IATSC	International Aeronautical Telecommunications Switching Center
ICAO	International Civil Aviation Organization
IFR	Instrument Flight Rules
IFSS	International Flight Service Station
ITS	Institute for Telecommunication Sciences
L Band	Frequency band ranging from 390-1550 MHz
LF	Low Frequency
MUF	Maximum Usable Frequency
NDB	Non-Directional Beacon

NOAA	National Oceanic and Atmospheric Administration
OCC	Oceanic Control Center
PCA	Polar Cap Absorption
SEL	Space Environment Laboratory
SELCAL	Selective Calling
SID	Sudden Ionospheric Disturbance
S/N	Signal-to-Noise Ratio
SOLTERWARN	SolarTerrestrial Warning
SST	Supersonic Transport
TTY	Teletype
TWEB	Transcribed Weather Broadcast
U.S.	United States
VHF	Very High Frequency
VOR	VHF Omnirange
VORTAC	VOR and Tactical Air Navigation
WPM	Words Per Minute
WMSC	Weather Message Switching Center

USCOMM - ERL